EVALUATION OF RELAP5 REACTOR CORE MODELING CAPABILITY

By

VINCENT J.-P. ROUX

A THESIS PRESENTED TO THE GRADUATE SCHOOL
OF THE UNIVERSITY OF FLORIDA IN PARTIAL FULFILLMENT
OF THE REQUIREMENTS FOR THE DEGREE OF
MASTER OF SCIENCE

UNIVERSITY OF FLORIDA

2001

To Lucie

ACKNOWLEDGMENTS

This research would not be completed without the contributions of several people. I would like to thank Dr. Samim Anghaie for his support and his wise advice throughout the project. His trust and guidance made my master's degree more than an academic experience. I would like to express my thanks to everyone who took the time to help me; especially Dr Gary Chen, whose experience and availability I value. Dr. Chris Allison and Dr. Alexandre Ezzidi were also ready to help me every time I needed it. I would also like to thank Dr. Edward T. Dugan and Dr. Rajat Mittal for their quality teaching and for taking the time to be on my supervisory committee.

I would like to thank my parents and my sisters Hélène and Cécile for their understanding and their support. I would also like to express my thanks to the French team. Their support and encouragement helped me to complete this research. I also thank all my friends in the department and at INSPI who made me enjoy my stay at the University of Florida. I am also grateful to Lynne, Denielle and Hélène for reviewing my work.

TABLE OF CONTENTS

page

ACKNOWLEDGMENTS iv

LIST OF TABLES vii

LIST OF FIGURES viii

1 INTRODUCTION 1

2 SYSTEM MODELING WITH RELAP5 4

About RELAP5 4
Capabilities of RELAP5 5
Physical Models and Numerical Methods 6
Conservation equations 6
Numerics 8
Cross-flow modeling 14
Comparing RELAP5 Core Model with and without Crossflow 14
Hydrodynamic Components 15
Core 15
Steam generator 18
Pressurizer 22
Primary cooling system tubing 24
Heat Structures 26
Heat structures in the core 26
Heat structure in the loop 28
Heat structures in the steam generator 28
Steady State and Initialization Process 29

3 PROTOCOL OF EVALUATION OF CROSS-FLOW MODEL USING HIGH RESOLUTION COMPUTATIONAL FLUID DYNAMICS 33

About FLUENT 33
General Overview 34
Basic Physical Models 35
Numerical Solvers 37
Numerical schemes and discretization 37
Boundary conditions 39
User defined functions 41

Turbulence Modeling in FLUENT 42
One-equation Spalart-Allmaras model 46
Two-equation k-epsilon model. 46
Defining a CFD Method for Evaluating RELAP5 Cross-Flow Model 48
FLUENT Model 49
GAMBIT grid generation 50
Boundary and operating conditions 51
RELAP5 Equivalent Model 53

4 CROSS-FLOW CHARACTERIZATION AND EVALUATION OF RELAP5 MODEL 55

Surry Reactor Calculation for a Steady State and a Simulated Power Surge Transient 55
Steady State 55
Transient Case: Simulation of a Power Surge Transient 60
Cross-flow Between Two Adjacent Channels: FLUENT and RELAP5 Results 64
Simulation in a Large-Diameter Vertical Pipe 65
If no power is added to the fluid 65
If power is added to the fluid 70
Simulation in a Small-Diameter Pipe 73
If no power is added to the fluid 73
If power is added to the fluid 76
Steam flow 76
Conclusions and Recommendations 78

APPENDICES

A SUMMARY OF SCDAP/RELAP5 HYDRODYNAMIC COMPONENTS 80

B RELAP5/SCDAP HEAT STRUCTURES FOR THE CORE AND STEAM GENERATOR 83

C RELAP5 INPUTS FOR THE TWO-CHANNELS SYSTEM 84

LIST OF REFERENCES 86

BIOGRAPHICAL SKETCH 88

LIST OF TABLES

Table		Page
2-1	Fuel rod power distribution.	27
4-1	Comparison of axial junction mass flow for a core with and without cross-flow.	56
A-1	Hydrodynamic components used to build the reactor model.	80
A-2	Hydrodynamic components in the steam generator	81
A-3	Hydrodynamic components of the primary loop.	81
A-4	Hydrodynamic components of the pressurizer.	82
B-1	Heat structures in the core and the steam generator.	83

LIST OF FIGURES

Figure		Page
2-1	Difference equation nodalization schematic.	9
2-2	RELAP5 nodalization diagram of the Surry reactor core.	17
2-3	RELAP5 nodalization diagram of a U-tube steam generator.	20
2-4	RELAP5 nodalization diagram of the pressurizer on the hot leg.	23
2-5	RELAP5 nodalization diagram of the primary cooling system tubing.	25
2-6	Bundle matrix for the first channel: 1 is a fuel rod – 2 is a control rod.	28
2-7	Evolution of the temperature distribution during the steady state run.	30
2-8	Axial coolant temperature distribution the steady state.	31
2-9	Radial fuel temperature profile at the sixth vertical node (height=2.012 m).	32
3-1	Mixing-length distribution in wall boundary layers.	45
3-2	Basic geometry studied with RELAP5 and FLUENT.	49
3-3	FLUENT calculation domain of the system.	49
3-4	Nodalization diagram of the equivalent RELAP5 model.,	54
4-1	Cross-flow magnitude versus height in the core for a total power of 2443MW.	57
4-2	Cross-flow mass flux versus core cell height.	58
4-3	Ratio of cross-flow to axial flow for different power levels and for different height in the core.	59
4-4	Power transient simulated in the transient test.	61
4-5	Cross-flow magnitude versus height in the core for a total power of 3500MW.	61

4-6 Cross-flow to inlet flow ratio for a 1000MW_{th} case. Cross-flow is from Channel 1 to 2.....62

4-7 Cross-flow to inlet flow ratio for a 2443MW_{th} case. Cross-flow is from Channel 1 to 2.....63

4-8 Two-sub channel pipe studied with FLUENT and RELAP5.....64

4-9 Inlet velocity profiles used in cross-flow simulation.....65

4-10 Axial evolution of the axial velocity profile. z is the height in meters.....66

4-11 Radial (V-velocity) and axial (U-velocity) velocity distribution at the entrance of the tube for V_i=6.0 m/s and V_o=2.0 m/s.....67

4-12 Radial (V-velocity) and axial (U-velocity) velocity distribution at the entrance of the tube for V_i=4.0 m/s and V_o=2.0 m/s.....67

4-13 Comparison of cross-flow prediction between FLUENT and RELAP for two simulations.....68

4-14 Evolution of the axial velocity for the two RELAP5 axial channels along the pipe, for the two inlet boundary conditions (a) and (b).....69

4-15 Temperature distribution over the total length of a 20.0 m pipe heated in the central channel at 66.1 MW/m^3.....70

4-16 Radial velocity for a constant inlet velocity and a heated central channel.....71

4-17 Cross-flow velocity at the artificial interface between the two channels.....72

4-18 Axial velocity in Channel 1 (heated) and Channel 2 (non-heated).....72

4-19 Radial velocity in a small size tube in an adiabatic flow. V_i=4.0 m/s and V_o=2.0 m/s.....74

4-20 Axial velocity in a small size tube in an adiabatic flow. V_i=4.0 m/s and V_o=2.0 m/s.....74

4-21 Cross-flow velocity versus distance to diameter ratio for large and small diameter tubes.....75

4-22 Cross-flow velocity for unheated small diameter channels (RELAP5 calculations).75

4-23 Cross-flow velocity between heated small diameter channels.....77

4-24 Axial velocity distribution for superheated steam.....77

Abstract of Thesis Presented to the Graduate School
of the University of Florida in Partial Fulfillment of the
Requirements for the Degree of Master of Science

EVALUATION OF RELAP5 REACTOR CORE MODELING CAPABILITY

By

Vincent J.-P. Roux

August 2001

Chairman: Professor Samim Anghaie
Major Department: Nuclear and Radiological Engineering

RELAP5 is a one-dimensional reactor-system simulation code with additional cross-flow calculation capability to include two- and three-dimensional effects in light water nuclear reactor cores. The code is used to model the core, steam generator, and the balance of the Surry reactor, which is a three-loop Westinghouse Pressurized Water Reactor (PWR) system. A detailed RELAP5 model including full nodalization of the system is developed and implemented for this study. The RELAP5 Surry core model uses one or several parallel channels to compare and assess the performance of the cross-flow model. Several inlet flow rates and core power distributions are considered and modeled. Results of the analysis showed the significant contribution of cross-flow in overall temperature and flow distributions in the core. Results of the study also showed that the RELAP5 predictions of cross-flow, at least for single-phase cases, are not consistent with the theory.

To evaluate the accuracy of RELAP5 cross-flow model, an industry standard Computational Fluid Dynamics code, FLUENT, is used to perform two- and three-dimensional calculations. Initial and boundary conditions for the RELAP5 model are used to develop a high-resolution FLUENT model for a pair of parallel reactor core channels. Two models were developed for FLUENT calculation of cross-flow. The first model is a simple tube with axisymmetric non-uniform inlet flow velocities. The second model included different power generation rates in the inner tube and the outer annulus. Results of flow rate in the transverse direction were compared with RELAP 5 cross-flow calculations under similar geometry and boundary conditions. All FLUENT calculations were performed using simple orthogonal mesh, however with a finer mesh in the regions of interest. The k-epsilon turbulence model is used to calculate turbulent viscosity. The power density is adjusted to account for the uniform heat generation inside the core.

Results of this study show the limitations and shortcomings of the RELAP5 to account for three-dimensional flow phenomena using the cross-flow model. The coarse mesh nodalization used in RELAP5 model limits the accuracy and resolution of cross-flow calculation. Results of RELAP5 calculation for different inlet flow conditions show the inadequacy of the simplified cross-flow model for predicting complicated two- and three-dimensional flow phenomena.

CHAPTER 1
INTRODUCTION

Research and development in the nuclear field is always active to create a new generation of safer and safer reactors. For simplicity of operating procedures and also to optimize the efficiency of the reactors, people try to understand more and more in detail all the phenomena that can occur in a reactor core. Researchers develop models to represent and calculate the behavior of the core in any situation to be able to know exactly the state of the reactor, should a problem occur; or even during normal operating conditions. A nuclear reactor is a complex entity that requires knowledge in neutronics, thermalhydraulics, chemistry, but also automated systems, informatics to develop the control system of the reactor. This study focuses on the thermalhydraulic characteristics and behavior of the reactor core. Many codes have been developed to predict temperature distribution in the core and pressure field intensity. An accurate mapping of the flow paths is useful to calculate heat removal capabilities, stresses inside the reactor, efficiency of the reactor, and safety features. Also from a neutronics point of view, flow path can be important, especially for two-phase flows. This will help in the design of new reactors. It is important to make sure that no component in the core reaches its melting point. Among all these tools, RELAP5 is one of the most popular and most widely used codes to do calculation of in-core parameters and to simulate reactor transients in Light Water Reactors (LWR). It allows for the modeling of the entire reactor and performs

calculations with an excellent accuracy. The entire nuclear community recognizes its performance.

However, numerical codes like RELAP5 need closure relations to solve the system of governing equations. Physical models adapted to a numerical treatment need to be used. These models, based on theoretical relations or empirical observations, are continuously improving. This study focuses on the cross-flow phenomenon. Crossflow is a well-known phenomenon, and extensive literature is available to show experimental observations and attempts to model this specific type of flow. By definition, the term “cross-flow” designates the fluid moving in a direction that is not the one of the main stream. Both streams do not necessarily have a direct interaction with each other. Cross-flow can be found in heat exchangers, for example. If the system is designed so that the cooling fluid is flowing around the tube bundle of the primary system in a normal direction, this is cross-flow cooling. However, the designation cross-flow is more commonly adapted to the flow of a jet mixing in another flow flowing in another direction. But these are cross-flows generated by geometry conditions, as analyzed by Wang (1). Cross-flow has been extensively studied considering jet mixers. This particular case concerns injection of fluid through a jet inside the main flow. Mixing velocity and turbulences generated are then studied (2). Computational Fluid Dynamics (CFD) tools allow calculating flow patterns, fluid velocities and turbulence parameters. By comparing experimental observations, turbulence models have been validated. A lot of work has been done to simulate flow path and the steady state velocity field of a cross-flow jet mixing in an axial stream. In a nuclear reactor core, cross-flow is due to grids and mixing devices, but also to inhomogeneous properties of the fluid. This phenomenon has a low

magnitude in a typical Pressurized Water Reactor (PWR) because the pumps, which impose a mass flux in the loop, drive the flow axially.

However, in case of natural circulation conditions, there is not the same strength anymore on the fluid, and then the flow is more sensitive to heterogeneity in the fluid properties. Sometimes, the problem can be much more difficult to handle. If the interest is in two-phase flow, then the modeling must be done very carefully because the difference of density between the two phases present is so large that buoyancy cannot be neglected and stress interaction between the two phases has to be carefully modeled. In a Boiling Water Reactor (BWR), cross-flow across the core is important. Cross-flow in a nuclear reactor core occurs between the different channels (or even sub-channels). If the peaking factors in the two adjacent channels, or assemblies are different, or if there is a grid mixer that makes the flow diverging from its path, it is important to understand what the effects of the cross-flow can be on the system. As illustrated by Kassera (3), cross-flow can induce tube vibration, which would be a serious concern in a nuclear reactor or in a steam generator, where the flow in the secondary loop is a mixture of two phases.

The purpose of this study is to analyze the efficiency of cross-flow modeling in RELAP5. The CFD calculation code FLUENT was used for this purpose. It has been useful to work on a simple system, and develop a model adapted for each of the codes. These models enhanced the cross-flow phenomenon, and a comparison of the results was performed. Finally, the calculations showed that there was a difference between RELAP5 and FLUENT cross-flow calculations. This thesis presents an actual simulation of a reactor, enhancing occurrence of cross-flow inside the core, and discusses the modeling of cross-flow in RELAP5, based on high-resolution CFD simulations.

CHAPTER 2
SYSTEM MODELING WITH RELAP5

In the modeling of cross-flow phenomenon, the first tool used was the thermalhydraulics code RELAP5. This code was developed to simulate a nuclear reactor coolant system during accidents as well as for normal operating conditions of the reactor. RELAP5 was used to simulate cross-flow phenomenon in a nuclear reactor core. First we present a brief description of RELAP5 capabilities. The model used for the calculation is based on the Surry reactor. The RELAP5 nodalization diagram of this reactor is explained in details in this chapter. Finally, the results of our simulation, emphasizing cross-flow behavior in the reactor core is presented.

The code RELAP5 was developed to simulate the behavior of a whole cooling system of the reactor. Even with a detailed description of the core's thermalhydraulic behavior, it is impossible to have a very high-resolution representation of the core. The whole reactor system was run to achieve a steady state and to achieve initial conditions for the CFD simulation.

About RELAP5

RELAP5 was used to simulate the whole core behavior during steady state and transient conditions. This code was developed for the U.S. Nuclear Regulatory Commission (US NRC) for transient analysis of light water reactors (LWR). The RELAP5 version used was provided by Dr. Chris Allison, from Innovative Software

System, Idaho Falls, Idaho (4). This version of the code is equipped with the severe core damage package SCDAP. The whole SCDAP/RELAP5/MOD3.2 package has a plot option that can plot evolution of any variable versus time, as requested. In the core model, SCDAP components will be used, however, no accident scenario will be calculated.

Capabilities of RELAP5

A specific use of RELAP5 is the simulation of transients in LWR systems. RELAP5 could, however, be applied for other kind of non-nuclear related thermalhydraulic system. This part shows the capabilities of the code RELAP5. The system's thermalhydraulic models are fully coupled at each time step. Hydrodynamics, heat conduction, reactor kinetics, control systems, trip logic and special component models, such as pumps or turbines will govern a RELAP5 case. Hydrodynamics is modeled by non-equilibrium, six-equation and two-fluid model. RELAP5 allows choosing an arbitrary number of volumes, junctions and surfaces. RELAP5 is a one-dimensional code; however, it can handle multiple-dimensional nodalization by using cross-flow junctions. Orthogonal direction then has to be specified. Heat transfer in RELAP5 is handled by 1D heat conduction theory for rectangular, cylindrical, or spherical geometry. An extensive heat transfer package is included in RELAP5 with the consideration of the effect of non-condensable gases. RELAP5 also takes radiative heat transfers into account. A reactor kinetics option is available in RELAP5. This task is performed by point kinetics theory or space dependent kinetics.

A control system in RELAP5 is performed by using different tools. The basic arithmetic operations are used to build the control system. It is also possible to use

differentiation and integration of variables to have a well-defined control system. Other direct control tools, such as standard or tabular functions can be used. To have an automated control system, trip logic operates the system. The variable trips are defined using arithmetic comparisons like “greater or equal” or “less than”… Logical trips were built with boolean operators "and," "or" and "xor." For instance, more developed logical trips are built in the code to control valve opening or pump motor velocity.

Physical Models and Numerical Methods

RELAP5 is a one-dimension thermalhydraulic code adapted for transient, two-fluid model. Thus, the code solves six equations of conservation as it simulates the two phases, liquid water and steam. Conservation equations of mass, momentum and energy are solved by RELAP5 for each phase. These equations are inter-related with each other. The eight primary independent variables considered in these equations are pressure (P), phasic specific internal energies (U_g and U_f), void fraction (α_g), phasic velocities (v_g and v_f), noncondensable quality (X_n) and boron density (ρ_b). Independent variables are time (t) and distance (x). There are also secondary dependent variables such as phasic densities (ρ_g and ρ_f), phasic temperatures (T_g and T_f), saturation temperature (T^S) and noncondensable mass fraction in noncondensable gas phase (X_{ni}). The nomenclature used is the same as in the RELAP5 Code Manual (5).

Conservation equations

The following are the conservation equations solved in RELAP5. The momentum equations are not modified when noncondensable species are present, however energy

equations are slightly modified and consider heat transfer at the noncondensable gas-liquid interface. These are the terms in {-} in the equations.

1. Vapor mass conservation: $\frac{\partial}{\partial t}\left(a_g r_g\right)+\frac{1}{A}\frac{\partial}{\partial x}\left(a_g r_g v_g A\right)=\Gamma_g$

2. Liquid mass conservation: $\frac{\partial}{\partial t}\left(a_f r_f\right)+\frac{1}{A}\frac{\partial}{\partial x}\left(a_f r_f v_f A\right)=\Gamma_f$

3. Vapor momentum conservation:

$$a_g r_g A\frac{\partial v_g}{\partial t}+\frac{1}{2}a_g r_g A\frac{\partial v_g^2}{\partial x}=$$
$$-a_g A\frac{\partial P}{\partial x}+a_g r_g B_x A-\left(a_g r_g A\right)FWG\left(v_g\right)+\Gamma_g A\left(v_{gI}-v_g\right)$$
$$-\left(a_g r_g A\right)FIG\left(v_g-v_f\right)-Ca_g a_f r_m A\left[\frac{\partial\left(v_g-v_f\right)}{\partial t}+v_f\frac{\partial v_g}{\partial x}-v_g\frac{\partial v_f}{\partial x}\right]$$

4. Liquid momentum conservation:

$$a_f r_f A\frac{\partial v_f}{\partial t}+\frac{1}{2}a_f r_f A\frac{\partial v_f^2}{\partial x}=$$
$$-a_f A\frac{\partial P}{\partial x}+a_f r_f B_x A-\left(a_f r_f A\right)FWF\left(v_f\right)-\Gamma_g A\left(v_{fI}-v_f\right)$$
$$-\left(a_f r_f A\right)FIF\left(v_f-v_g\right)-Ca_f a_f r_m A\left[\frac{\partial\left(v_f-v_g\right)}{\partial t}+v_g\frac{\partial v_f}{\partial x}-v_f\frac{\partial v_g}{\partial x}\right]$$

5. Vapor energy conservation:

$$\frac{\partial}{\partial t}\left(a_g r_g U_g\right)+\frac{1}{A}\frac{\partial}{\partial x}\left(a_g r_g U_g v_g A\right)=$$
$$-P\frac{\partial a_g}{\partial t}-\frac{P}{A}\frac{\partial}{\partial x}\left(a_g v_g A\right)+Q_{wg}+Q_{ig}+\Gamma_{ig}h_g^*+\Gamma_w h_g^{'}+DISS_g\ \left\{-Q_{gf}\right\}$$

6. Liquid energy conservation:

$$\frac{\partial}{\partial t}\left(a_f r_f U_f\right)+\frac{1}{A}\frac{\partial}{\partial x}\left(a_f r_f U_f v_f A\right)=$$
$$-P\frac{\partial a_f}{\partial t}-\frac{P}{A}\frac{\partial}{\partial x}\left(a_f v_f A\right)+Q_{wf}+Q_{if}+\Gamma_{ig}h_f^*+\Gamma_w h_f^{'}+DISS_f\ \left\{+Q_{gf}\right\}$$

7. Noncondensable component mass conservation:

$$\frac{\partial}{\partial t}\left(a_g r_g X_n\right)+\frac{1}{A}\frac{\partial}{\partial x}\left(a_g r_g X_n v_g A\right)=0$$

8. Boron concentration in the liquid field:

$$\frac{\partial r_b}{\partial t}+\frac{1}{A}\frac{\partial}{\partial x}\left(a_f r_f C_b v_f A\right)=0$$

Numerics

Spatial discretization of the set of differential equations is performed by integrating the differential equations over the cell volume for the volume quantities (that define scalar properties like pressure, energies and void fraction), and between cell centers for junction quantities (representing vector quantities like velocities). Figure 2-1 shows the typical spatial noding resulting from this definition (5). This approach results in a numerical scheme having a staggered spatial mesh. Numerically there should not be an ill-posed problem; RELAP5 uses different techniques to get rid of instability problems for mesh sizes of practical interest. This is done by avoiding explicit treatment of time advancement. Two possible time advancement schemes are available in RELAP5. Each of them is more or less adapted to a specific case. For instance, it will be more adapted to use a nearly implicit scheme for a steady-state or self-initialization case problem where the time step is limited by the Courant limit, but also for slow phases of a transient problem. Basically, a semi implicit time advancement scheme is adapted for transient runs. The principle of the semi-implicit scheme is to replace the system of partial differential equations with a system of finite-difference equations partially implicit in time. For the semi-implicit solution strategy, seven simultaneous equations are to be solved: two per junction and five per volume. The five density and energy variables are

expressed as differences (in time) and are ordered, $\Delta X_{n,i}=X_{n,i}^{m+1}-X_{n,i}^{m}$, $\Delta u_{g,i}=u_{g,i}^{m+1}-u_{g,i}^{m}$, $\Delta u_{f,i}=u_{f,i}^{m+1}-u_{f,i}^{m}$, $\Delta a_{g,i} = a_{g,i}^{m+1} - a_{g,i}^{m}$ and $\Delta P_i = P_i^{m+1} - P_i^{m}$, m is the time index. Junction unknowns are velocities $v_{g,j}^{m+1}$ and $v_{f,j}^{m+1}$ for the junction j.

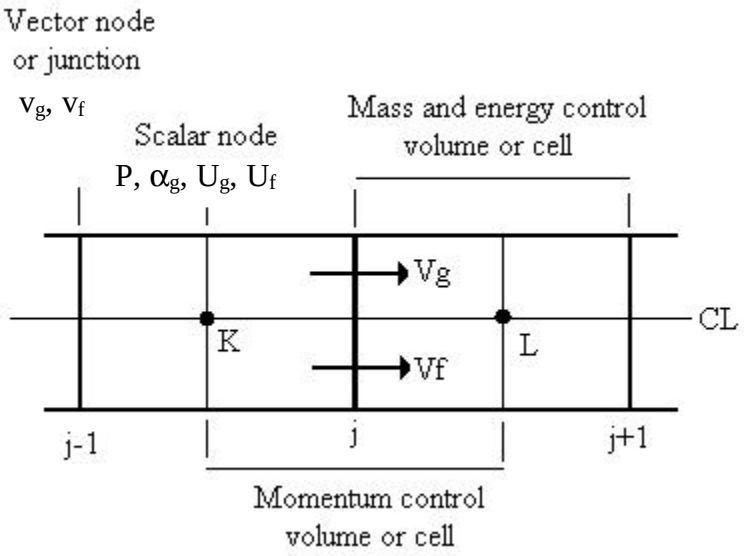

Figure 2-1: Difference equation nodalization schematic.

For each junction, the only unknowns involved are the velocities and the pressure of the volumes connected by the junction. The tilde (~) sign is used to specify that the term is a matrix type term. All terms in these matrices are calculated using "old time" values. Components of the vector $\tilde{v}_j^{m+1}$ are the gaseous and liquid phase velocities at junction j at time m+1.

$$\tilde{B}_j \tilde{v}_j^{m+1} = \left(P_k^m + \Delta P_k\right) - \left(P_l^m + \Delta P_l\right) + \tilde{r}_b$$

For each junction, we have a two-equation system easily solved in term of the pressure change, however it is not yet possible to get a value for the new pressure, nor the new velocity.

$$\tilde{v}_j^{m+1} = \tilde{B}_j^{-1}\left(\Delta P_k^{m+1} + \Delta P_l^{m+1}\right) + \tilde{B}_j^{-1}\tilde{r}_b$$

The five other volume equations can be written in an order-five matrix form. Fortunately, the unknowns for each volume equation involve only the unknown quantities for this given volume and the velocities for the junctions attached to the volume. And so, for each volume i,

$$\tilde{A}_i \tilde{\Delta}_i = \tilde{b} + \sum_{j \in i} \left(\tilde{g}_i \tilde{v}_{g,j}^{m+1} + \tilde{f}_i \tilde{v}_{f,j}^{m+1} \right)$$

with $\tilde{\Delta}_i = \begin{bmatrix} \Delta X_{n,i} \\ \Delta u_{g,i} \\ \Delta u_{f,i} \\ \Delta a_{g,i} \\ \Delta P_i \end{bmatrix}$ and $\tilde{A}_i$ is the order five matrix of the system. The detail of the terms in these equations can be obtained in the RELAP5 user manual (5). Thus, the five equations allow the volume quantity for each volume to be written in terms of the velocities in the attached junctions. Then from the previous comment, at this point only the ΔP_i solution is needed. The matrix A_i is then factorized into lower and upper triangular matrix (A_i=LU), and from these, the bottom row of the inverse A_i^{-1} is computed. It can be shown that this particular row represents an equation involving only the pressure in the volume and the velocities in the attached junction:

$$\Delta P_i = A_{51,i}^{-1} \left(b_{1,i} + \sum_{j \in i} g_{1,j} v_{g,j}^{m+1} \right) + A_{52,i}^{-1} \left(b_{2,i} + \sum_{j \in i} g_{2,j} v_{g,j}^{m+1} \right) + A_{53,i}^{-1} \left(b_{3,i} + \sum_{j \in i} f_{3,j} v_{f,j}^{m+1} \right) +$$
$$A_{54,i}^{-1} \left(b_{4,i} + \sum_{j \in i} \left(g_{4,j} v_{g,j}^{m+1} + f_{4,j} v_{f,j}^{m+1} \right) \right) + A_{55,i}^{-1} \left(b_{5,i} + \sum_{j \in i} \left(g_{5,j} v_{g,j}^{m+1} + f_{5,j} v_{f,j}^{m+1} \right) \right)$$

This equation involves only the pressure in the volume and the velocities in the attached junctions. Substituting the velocity expressions previously obtained from the junction equations into this expression, the resulting expression involves the ΔP for the volume i and the ΔP's for each volume connected to this volume by the attached junctions. So

combining the ΔP equation for each volume leads to a system of simultaneous equations, one per volume. And,

$$\tilde{\tilde{C}}\Delta\tilde{\tilde{P}} = \tilde{\tilde{r}}_p$$

For a strictly one-dimensional pipe, the matrix $\tilde{\tilde{C}}$ is tridiagonal. A typical reactor system with loops and branches would not have a regular pattern, but a proper ordering of the equations would show sub matrices of tridiagonal and two-dimensional form. This system is solved and the ΔP's obtained from the pressure equations are directly substituted into the two velocity equations for each junction, thus obtaining the velocities. The ΔP's and velocities are substituted into the remaining four equations (out of the original five) for each volume. These four equations are actually solved for $\Delta X^*_{n,i}$, $\Delta u^*_{g,i}$, $\Delta u^*_{f,i}$ and $\Delta a^*_{g,i}$ which are the unknown values at a provisional "new time". The actual "new time" variables $\Delta X_{n,i}$, $\Delta u_{g,i}$, $\Delta u_{f,i}$ and $\Delta a_{g,i}$ are determined using the unexpanded difference equations (5). Note that instead of solving a set of two equations per junction plus five equations per volume, the semi-implicit technique allows solving an order two system for each junction, an order five system for each volume, and one system of one equation per volume. This was possible by using new or old time values for hydrodynamic unknowns. This technique is characterized by using only old time values for convection quantities. The semi-implicit method limits the time step to the Courant limit. The Courant limit is a parameter equal to the ratio of the length of the cell to the velocity of the fluid in the cell. This numerical limitation has a physical meaning. By limiting the time step to the Courant limit, it does not allow fluid to travel a path longer than the cell itself during the time step. The nearly implicit method is not limited

by Courant limit. The basic idea of the nearly implicit scheme is to split the equations into fractional steps based upon physical phenomena.

This scheme consists of two major steps to avoid solving the complete set of two equations per junction and five equations per volume. The first solves all conservation equation in the expanded form, as for the semi-implicit method. It results in one equation per volume involving the ΔP_i for the volume i and the velocities of the junctions attached to this volume. Convective terms in the momentum conservation equations (junction equations) are treated implicitly, meaning that the scheme uses new time values. The resultant equations involve the velocities in junction j and the ΔP 's from the volume k and l connected by junction j (Figure 2-1) as in the semi-implicit technique, but also involve the velocities from each junction connected to volumes k and l. The simple solution of the order two matrices for the velocities in terms of the pressure changes is no longer possible and the substitution of the velocity expressions into pressure equation is likewise not possible. Instead, substitute the pressure equation into the velocity equations. The resultant two equations for each junction involve $v_{g,j}$ and $v_{f,j}$ and the velocities for each junction connected to the volumes k and l. Combining these two equations per junction leads to a set of simultaneous equations involving only the velocities. The shapes of the matrix for the semi-implicit technique and this stage of the nearly implicit step have similarities. The junction equations are solved using the same sparse matrix solver as used in the semi implicit technique. The velocities are substituted into the five equations for each volume, and each order five system is solved for the volume quantities $\Delta\tilde{X}_{n,i}, \Delta\tilde{u}_{g,i}, \Delta\tilde{u}_{f,i}, \Delta\tilde{\alpha}_{g,i}$ and ΔP_i. At this point, we do not obtain "new time" values. The

tilde (~) symbol on the top of the first four quantities indicates that these are not the final value for these quantities.

The second step consists of solving the unexpanded form of the mass and energy equation. Using the final values for the velocities and pressure changes, and the intermediate values for the noncondensable mass fractions, internal energies, and void fractions, the phasic conservation of mass and conservation of energy equations are written with the convective quantities now at new time values. Interphase quantities such as interphase mass transfer are evaluated using the linearized equations with intermediate results. For a volume, each phasic equation involves only one type of unknown. Vapor noncondensable equation involves only $(\alpha_g \rho_g X_n)^{m+1}$, vapor mass equation involves only $(\alpha_g \rho_g)^{m+1}$, liquid mass equation involves only $(\alpha_f \rho_f)^{m+1}$, vapor energy equation involves only $(\alpha_g \rho_g u_g)^{m+1}$ and liquid energy equation involves only $(\alpha_f \rho_f u_f)^{m+1}$. An equation for a volume involves the convected terms for that volume and convected terms from the volumes connected by the attached junctions. As five sets of simultaneous equations result from gathering the same type of equation for every volume, the shape of these five matrices are the same and have the same shape as the pressure matrix $\tilde{C}$ in the semi-implicit scheme. The terms X_n^{m+1}, u_g^{m+1}, u_f^{m+1} and α_f^{m+1} are obtained by dividing between each other's previous five terms. ρ_f^{m+1} is obtained from linearized equation of state using P^{m+1} and u_f^{m+1}.

A detailed description of the two methods is extensively presented in the first volume of the RELAP5 code manual (5).

Cross-flow modeling

As RELAP5 is a one-dimension code, a specific model is used to calculate cross-flow, which by definition, is occurring in the normal direction to the main direction of the flow. For small cross-flow between reactor core channels, simplified cross-flow momentum equations are used to couple two adjacent channels linked with a cross-flow junction. In the momentum equation, the transverse momentum advection terms are neglected, meaning that there is no transport of x-direction momentum due to flow in the transverse direction. Cross-flow areas can be entered or calculated by the code. If the code has to calculate the junction area, it considers the geometry of a cylindrical pipe. Detailed governing equations for modeling of cross-flow phenomenon are presented in the user's manual (5).

Comparing RELAP5 Core Model with and without Crossflow

Calculations were performed with the model of the Surry reactor. The Surry Nuclear Plant is located in Norfolk, Virginia. It has two Westinghouse 3-Loop PWR reactors. Each unit is rated 823 MWe (2443 MW_{th}). Surry is owned and operated by Virginia Power. Each loop is composed of a steam generator, a pump and a tubing system. One of them has a pressurizer on the hot leg. An accumulator is also present on every loop on the cold leg, for the emergency cooling system. The following description presents these elements: the core, the steam generator, the pressurizer and the tubing related to the primary loop. For each element, a picture of the nodalization diagram and the initial conditions for temperatures and flow rates in the cells and junctions are given. Also this paper describes the heat structures that are used to model the heat transfer

characteristics inside the core and along the loops and also are used to model the power generation in the core. A detailed description of the input requirements can be found in the Appendix A of the SCDAP/RELAP5/MOD3.2 user's guide and input manual (6).

Hydrodynamic Components

The reactor model is mainly composed of hydrodynamic components that basically represent the parts of the reactor where coolant passes through and heat structures that represent solid parts of the reactor (there is no flow in the heat structures) where also heat can be generated or conducted to other regions of the reactor or the environment. The following is a presentation of the different parts of the reactor modeled in this problem.

Core

Figure 2-2 shows the nodalization diagram of the core. This is a five-channel core model. The core is composed of a downcommer (104) coming to the lower head (106) and the lower plenum (108). The fueled part of the core is composed of five channels (111, 112, 113, 114 and 115) and a bypass region (118). The upper plenum of the core is only a 3-channel model ([151-152-153-154], [161-162-163-164] and [171-172-173-174]). The control assembly housing is represented in three parts (181, 182 and 183). The upper head (190) is covering the core. Upper annulus (100) and inlet annulus (102) are also represented in this model. This is a quite detailed nodalization scheme. It can be useful to describe and analyze cross-flow phenomenon. Inlet annulus (component 102) is the hydrodynamic volume where cold coolant enters the core. Junctions with upper annulus (100) and upper plenum (172) are considered, but surface junctions are much

smaller than with the downcommer (104), meaning that most of the flow will go down the downcommer. Also initial junction coolant velocities are set in consequence. The downcommer is represented by a pipe and divided into seven cells. Initial conditions for these cells are pressure and temperature. Pressure is calculated to take into account the gravity effects (from 2286.0 psi for the upper cell to 2290.5 psi for the lower cell). Temperature is essentially constant throughout the downcommer and about equal to 543.0 °F. The lower head (106) is a branch-type hydrodynamic component. Pressure and temperature are given in this branch and equal to 2294.4 psi and 543.02 °F. Initial liquid and vapor velocities in the junctions are given. The lower plenum is described the same way as the lower head. Inlet loss coefficients are set to 8.0 for each channel (bypass and core channels). Inlet liquid velocity is 13.4 ft/s in the core channels and 8.4 ft/s in the bypass region. The core channels are modeled with pipe components. The only difference between them is the volume flow area of the cells. Initial pressure is 2275.0 psi in all the cells and 577.0 °F. Fluid velocities are given at the junctions (14 ft/s). Ten cells of identical size are used to model the length of the channel (12 feet long heated rods). Heat structures associated to these hydrodynamic volumes will be described later. As represented on the diagram, cells of different channels are interconnected with each other using single cross-flow junctions:

- Components 140-149 connect the center core Channel 1 and center core Channel 2.
- Components 120-129 connect the center core Channel 2 and the middle core Channel 3.

- Components 80-89 connect the middle core Channel 3 and the middle core Channel 4.
- Components 130-139 connect the middle core Channel 4 and the outer core Channel.

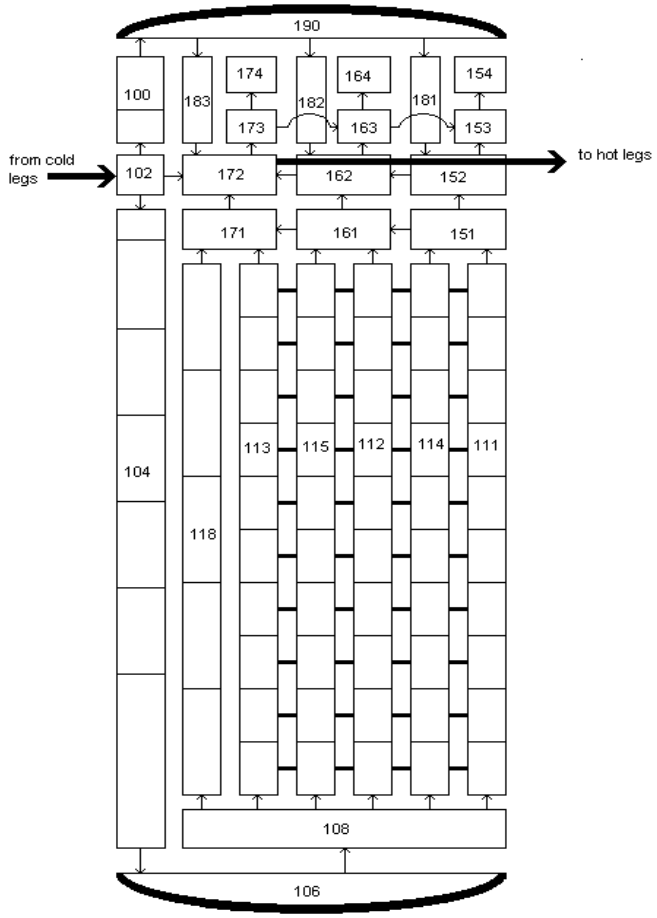

Figure 2-2: RELAP5 nodalization diagram of the Surry reactor core.

Initial velocities for all junctions between the channels are set to zero. There is no junction between the bypass region and the center channels. In the case of calculation without cross-flow, the four sets of cross-flow junctions are not included. The flow is not able to pass from one channel to the other. The bypass region is modeled by a five cell-

pipe. Pressure in assumed to be 2276.0 psi and temperature 543.2 °F. Initial velocity at the four inner junctions is 0.8124 ft/s. The upper plenum is composed of branch components, which allow cross-flow in the upper part of the core and drive the flow of coolant to the outlet of the core (hydrodynamic component 172). Junction between the heated channels and the upper-plenum (volume 151, 161 or 171) induces energy flow losses. The loss coefficient is equal to 8.0 for the outlet effect of the channels. Energy losses are also considered in the transversal direction (coefficient equal to 5.0 for the junctions 151-161 and 152-162 and 7.0 for the junctions 161-171 and 162-172). The inverted hat of the upper head has been represented using branch components (153-154, 163-164 and 173-174). In each of these components, initial pressure is equal to 2250.0 psi and temperature to 606.0 °F. Housing for the control assembly is represented by single volume components (one for each upper head sub-channel, 181, 182 and 183). Pressure is set to 2250.0 psi and temperature to 550.0 °F. To cover all this and the core component, the Upper Head (190) is modeled using a branch component in order to take into account all the junctions with control assembly housing volumes. Initial pressure in the upper head is 2250.0 psi and temperature is 543.0 °F. It is considered that there is no loss between the upper head and the upper plenum and initial liquid velocity at the junction upper head/upper plenum is 1.0 ft/s. The flow is going down in the reactor as some flow is coming up from the upper annulus (100). Actually, this flow is really low.

Steam generator

Figure 2-3 represents the nodalization of the secondary side of one of the steam generators used in each of the loops. The primary side, represented only by U-tubes is described with the primary side tubing system. Radioactive water from the primary side

enters the steam generator at the bottom and flows through small diameter reversed U-tubes. This coolant looses its heat, which is transferred to the water of the secondary side coming from the steam generator feedwater and flowing outside the tubes. This system allows this non-radioactive water to get turned into steam and then, moist steam is produced and goes through the steam separator which provides dry steam to the steam outlet (this steam is then sent to drive the turbines) and remaining water is sent directly to the downcommer of the steam generator to be reheated. Finally, the superheated steam is distributed through valves present at the outlet of the steam generator dome. The steam generator feedwater is represented by a time dependent volume (266) where the initial conditions for water supply are 785.0 psi and 430.0 °F. The downcommer of the secondary side of the steam generator is comprised of three components, the hydrodynamic volumes (270, 272 and 274). The inlet volume is the branch 272 which receive water from the inlet feedwater, the upper volume 270 and the separator 278. Water coming from the separator is the result of the separation of steam and moisture to provide only dry steam to the turbines. Initial properties for the water in the volume 272 are a pressure of 832.13 psi, and specific internal energies of 495.85 Btu/lb for the liquid phase and 1114.42 Btu/lb for the vapor phase. A pipe divided into four cells models the main downcommer part. For these volumes, initial conditions are given by Pressure, liquid specific internal energy and vapor specific internal energy. Pressure calculation includes a gravity effect. Change in internal energy (for liquid or vapor) is not significant and is about 495.8 Btu/lb for the liquid and 1114.3 Btu/lb for the vapor phase. The pressure is 834.24 psi at the top of the pipe and 839.92 psi at the bottom of the pipe. The vertical pipe used to model the cavity surrounding the inverted U-tubes where water will

be boiled (276) is divided into five parts. For each of them, initial conditions on Pressure, specific internal energy for liquid and vapor phase are given. For this region, it is necessary to specify the hydraulic diameter, taking into account the number of tubes. This has been calculated and the hydraulic diameter of the component is 0.14 ft.

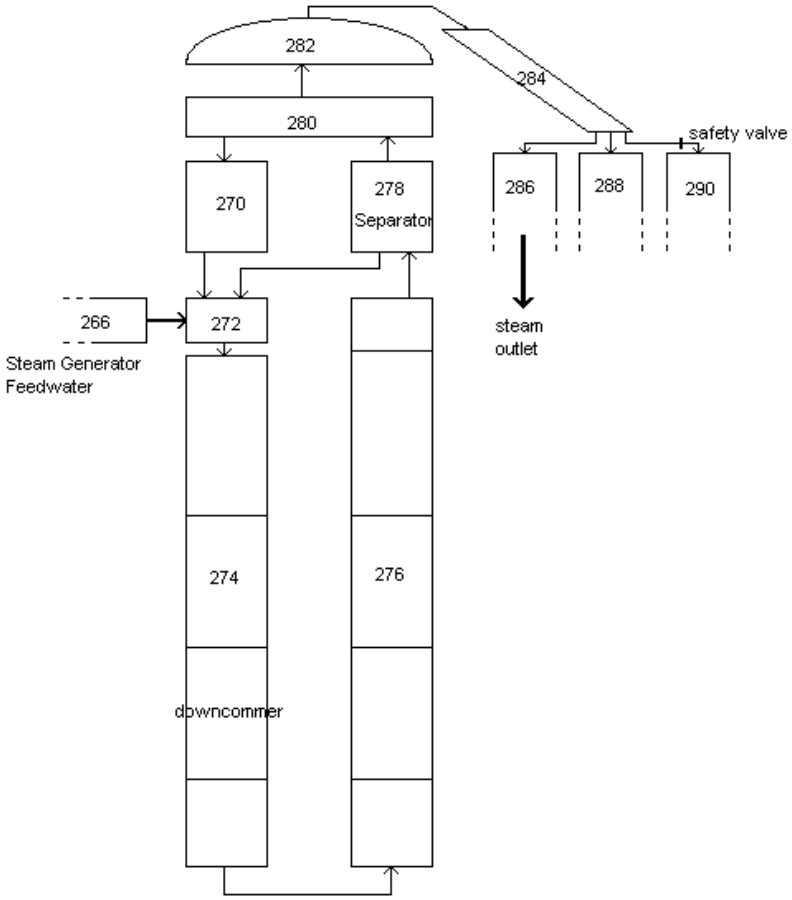

Figure 2-3: RELAP5 nodalization diagram of a U-tube steam generator.

Also energy loss coefficients are specified and equal to 16.9 at the first junction (which can represent the bottom of the bundle) and 6.0 for the middle region (the second and third junctions). No loss is considered in the last junction. The swirl vane moisture separator has a built-in model in the code, and this model is used to model the steam separator (278). The purpose of this component is to separate steam from liquid water

and send the latter back to the downcommer. Drying of the steam is performed in two stages so that an additional dryer is added (branch 280 in this model). The dryer is also connected to the downcommer to get rid of the excess liquid water. At the top of the unit, the steam generator Dome is represented by a single volume component. Initial conditions for the fluid in the dome are a Pressure of 830.16 psi, specific internal energies of 511.85 Btu/lb for the liquid phase and 1114.49 Btu/lb for the vapor phase. The vapor void fraction is very close to 1.0. The steam line connecting the steam dome to the different valves managing the steam distribution and the safety of the system is represented by the pipe 284. Three valves are present in the system. The purpose of each of them is well defined.

- The main valve (285) controlling the steam flow through the main steam line is represented with a servo-valve (model built in the code. The valve flow area is calculated by a control system). The initial velocities are set to 102.2 ft/s for the liquid phase (even if the quantity of liquid is much lower than the vapor one) and 115.6 ft/s for the vapor phase.
- The second valve (287) is called the porv “power operated relief valve”. A “motor valve” type valve models this valve. This valve opens if pressure in the dome steam line 284 gets greater than 1050.0 psi and closes when pressure in 284 has become less than 1000.0 psi. This valve is initially closed and the valve change rate is specified in the inputs. Initial velocity has to be set to zero as the valve is initially closed.
- The third one is a safety valve (289), which is also a motor valve. It opens when the pressure in 284 is higher than 1184.0 psi and closes when

pressure in 284 drops down below 1092.0 psi. Again, this valve is initially closed, but has a much higher junction area (which allows the pressure to decrease faster) and the valve change rate is about 40 times larger than the porv valve, which means faster opening ability. In term of rate of change of normalized valve area, the porv opens at a rate 0.556 s^{-1} whereas the safety valve opens at a rate 20.0 s^{-1}. Here again, the initial velocity is set to zero as the safety valve is closed in normal conditions of operation.

The opening of the valves is commanded by trips defined in the input file. With these trips, it is possible to build control variables (using basically logic statements to elaborate different trips).

Pressurizer

The Pressurizer is used to maintain a constant pressure in the primary cooling system. It is composed of a large tank. It is about half full of liquid water and the other half contains steam. The whole tank was designed to remain at constant pressure, and because it is connected to the primary system, it will regulate the pressure of the primary cooling system. Temperature in the pressurizer is a bit higher than the saturation pressure corresponding to the set pressure point. Electric heaters will be activated to vaporize a fraction of the liquid to increase the pressure in the pressurizer and in the loop, whereas sprays are designed to cool the vapor and condense it to decrease the pressure if needed. The tank of the pressurizer should never become totally full of water (it would then be impossible to decrease the pressure), or on the contrary full of steam (it would then be impossible to increase the pressure). Figure 2-4 shows the pressurizer on the hot leg of one of the loops. 172 is the outlet of the core. The Pipe 400 is the hot leg of the loop. The

branch will connect the pressurizer to the circuit. These elements will be described more precisely later. The Pipe 443 represents the surge line. Pressure in this pipe is initially taken as 2260.0 psi.

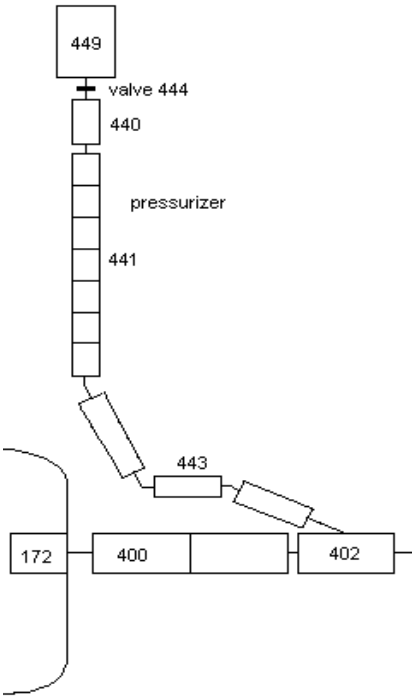

Figure 2-4: RELAP5 nodalization diagram of the pressurizer on the hot leg.

The pipe 441 represents the tank. The upper part of this tank, the pressurizer dome (440), is represented by a branch-type element. Two valves can connect the tank to a container represented by a single volume (449). The first valve (444), which is a motorvalve, would represent the spray nozzle intended to condense vapor in case of a need to reduce the pressure. This event would occur if the pressure becomes higher than 2350.0 psi and would stop when pressure goes lower than 2280.0 psi. The safety valve of the pressurizer is numbered 445 in the model. The safety valve is also considered to be a motorvalve. This valve opens when pressure in the tank becomes greater than 2575.0 psi and closes when the pressure drops back below 2375.0 psi. Although the safety valve

diameter is larger (about three times) than the pressurizer porv, both of them open at the same rate: 5.0 s^{-1} (the definition of the rate is also based on the normalized valve area). Initial mass flow rates through the valves are of course equal to zero.

Primary cooling system tubing

The primary loop shown on Figure 2-5 contains the primary side of the steam generator and a pressurizer (only one is necessary for the whole plant) on the hot leg and the pump and an accumulator (used as emergency cooling system) on the cold leg. The pressurizer has been previously described. The pump included in this system is the same for each loop. It is possible to use built in models of pumps usually used (Westinghouse for instance) or describe the characteristics of head and torque, pump head and torque multiplier, and two phase difference curve. The characteristics were entered in this input deck. The purpose of the accumulator is to act as an Emergency Core Cooling System (ECCS) if needed. The accumulator has a built-in model in the code, as it requires special numerical treatment. The geometry of the tank is needed, pressure (set at 615.0 psi), temperature (set at 120.0 °F) and tank initial fill conditions. Conditions are the same for the three systems. As stated previously, the hot leg is mostly composed of pipes. The pipe 200 going from the vessel to the pressurizer is a 2-cells 9.16 ft long pipe. Initial pressure is 2234.9 psi. The Branch 202 is used to connect the pressurizer to the hot leg. This branch is included on each leg, but only one of them, the 4XX has a pressurizer plugged on it. The Single Volume 204 is the inlet tube of the primary side of the steam generator. Initial conditions in all these tubes are given with the pressure, the specific internal energies for liquid and vapor phases and vapor void fraction. A single pipe represents the tube sheet of the steam generator on the primary side. The Branch 206 is used to connect

the Tube Sheet 208 to the inlet of the Steam Generator 204. The tube sheet is represented by the Pipe 208, which is divided into eight cells, so that it can represent the U-tube geometry (as shown on Figure 2-5).

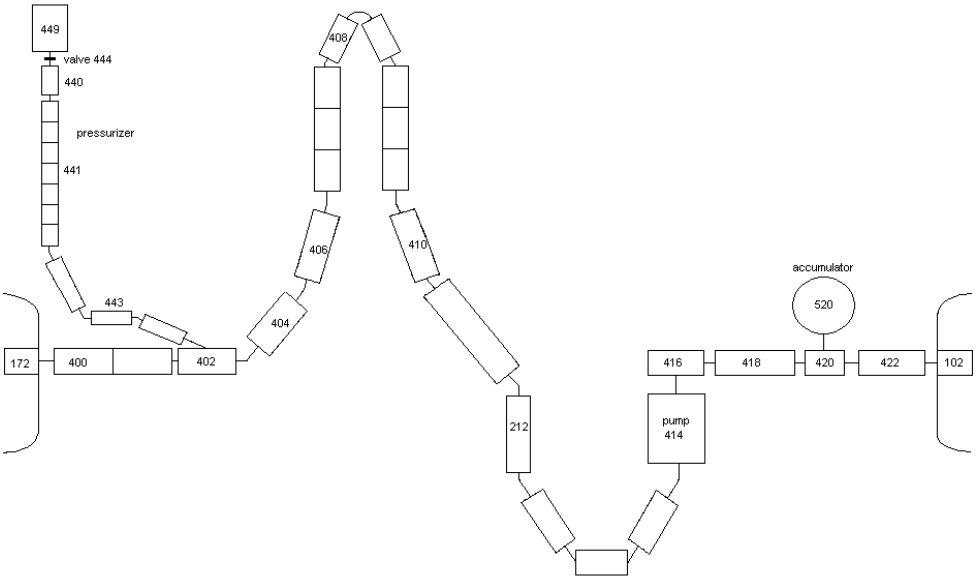

Figure 2-5: RELAP5 nodalization diagram of the primary cooling system tubing.

For all these cells, initial conditions are set with pressure (from 2232.2 psi for the inlet to 2170.4 psi for the outlet), taking into account the energy loss coefficients (0.048 at the junctions and 0.00015 for the wall roughness). Also, specific internal energies are given and the vapor void fraction is set to zero. A Branch 210 is used to connect the outlet of the steam generator primary side to the suction pipe of the reactor-cooling pump (212). This simple pipe is composed of four cells, which allow giving a realistic representation of the actual geometry of the system. The cold leg of the loop is represented by a series of branches and pipes. The pump is plugged right after the previously described Pipe 212 and sends water through a series of single volume components 216, 218 and 220 (where is located the ECCS). The inlet of the reactor is

done with a single volume component that joins the Cell 200 in the reactor. A complete summary of hydrodynamic components can be found in Appendix A.

Heat Structures

Heat structures in the core are of two types. The version of the code used is a modified version of RELAP5. This includes a specific version to treat severe accident. SCDAP/RELAP5 MOD3.2 allows fuel to melt and can model the relocalization of the molten fuel and can predict the quantity of hydrogen produced in case of oxidation of steam during LOCA. We obtained the code from ISS, Idaho Falls, Idaho. Different materials are used to model all the heat structures in the code. We entered them in some specific cards 201MMMNN for Heat Structures Material Properties.

Heat structures in the core

There are a lot of heat structures in the core. Especially, all the walls have conduction properties that cannot be neglected. All vessel walls, thermal shields (in addition to the vessel wall), different structures and plates present in the core to maintain the assemblies and the integrity of the vessel, the core barrel and the core baffle are modeled with heat structures. Geometrical models are to be chosen to model the heat conduction (rectangular, cylindrical or spherical geometry). Other information essentially needed are the heat structure mesh interval data, the composition of the structure, the boundary conditions on the right and left side of the structure and the initial temperature distribution. For all these heat structures no source of heat is used because the only power source of the reactor is the fuel. The fuel can be modeled by RELAP5 type inputs, or SCDAP inputs. SCDAP components were chosen. The fuel rods and control rods are

modeled using SCDAP components. For each channel (total of five), one component "Fuel" for the fuel rod and one component "Control" for the control rods and instrumentation tube are described. Information concerning radial mesh spacing in the rod component (the code has built in models for fuel rods), initial radial temperature distribution, power distribution, axially and radially, and information about the power history of the fuel are specified. For each fuel rod component, the number of fuel rods included in the model is specified. Table 2-1 shows the power fraction for each fuel rod component and the number of rods associated with this component.

Table 2-1: Fuel rod power distribution.

Component	Type	# of rods	Power fraction
1	Fuel	1020	0.04
2	Control	105	0
3	Fuel	4080	0.15
4	Control	420	0
5	Fuel	7344	0.24
6	Control	756	0
7	Fuel	12360	0.37
8	Control	1260	0
9	Fuel	7344	0.20
10	Control	756	0

The power fraction for each fuel element can be calculated knowing the number of rods modeled in each element and the power peaking factors associated to each fuel rod (or assembly). Radiation heat transfer option is activated in this study, so we have to input the bundle matrix so that the code can calculate the view factor for every channel. A typical bundle (here for the first channel) is described Figure 2-6.

1	1	1	1	1	1	1	1	1	1	1	1	1	1	1
1	1	1	1	1	1	1	1	1	1	1	1	1	1	1
1	1	2	1	1	2	1	1	1	2	1	1	2	1	1
1	1	1	1	1	1	1	2	1	1	1	1	1	1	1
1	1	1	1	2	1	1	1	1	1	2	1	1	1	1
1	1	2	1	1	1	1	1	1	1	1	1	2	1	1
1	1	1	1	1	1	1	1	1	1	1	1	1	1	1
1	1	1	2	1	1	1	2	1	1	1	2	1	1	1
1	1	1	1	1	1	1	1	1	1	1	1	1	1	1
1	1	2	1	1	1	1	1	1	1	1	1	2	1	1
1	1	1	1	2	1	1	1	1	1	2	1	1	1	1
1	1	1	1	1	1	1	2	1	1	1	1	1	1	1
1	1	2	1	1	2	1	1	1	2	1	1	2	1	1
1	1	1	1	1	1	1	1	1	1	1	1	1	1	1
1	1	1	1	1	1	1	1	1	1	1	1	1	1	1

Figure 2-6: Bundle matrix for the first channel: 1 is a fuel rod – 2 is a control rod.

Heat structure in the loop

Heat structure concerning hot leg piping is simply a cylindrical geometry with left boundary condition taken as the hydrodynamic volumes associated to the hot leg piping and “0” as right boundary condition, meaning that we consider zero gradient of temperature in the insulation of the pipe. Steam generator heat structures will be discussed in the following part even if it is really part of the primary loop. Cold leg piping and pump suction piping are also cylindrical geometry heat structures.

Heat structures in the steam generator

The heat structure of the steam generator is very complex due to the large number of support plates for the tubes, and also, heat transfer between primary and secondary sides need to be accurately modeled to represent the heat removal capability of the steam generator. It is a heat structure that does the thermal connection between Pipe 208 (the tube sheet of the primary side of the loop) and Pipe 276 (boiler part of the secondary side

of the steam generator). A cylindrical geometry is used with no heat generation inside the heat structure. For this particular case, heat transfer is treated as convective phenomenon at the boundary. The heat transfer coefficient can be calculated using a table that the user can enter. In this study, the convective heat transfer coefficients were calculated with the package included in the code. The secondary side of the steam generator also contains heat structure components for walls (shell top, upper shell, middle shell, shell base, lower shell) and for the wrappers (lower wrapper between 274 and 276) and upper wrapper and swirl vanes (between 276 and 278, and 272 and 270). Calculations of heat transfers through these components are also based on a cylindrical geometry. A summary of the heat structures used in this model can be found in Appendix B.

Steady State and Initialization Process

The initialization run is a "steady-state" type run. Nearly implicit time advancement has been chosen for the numerical time incrementation method. The power for this experiment is set and controlled by a power table and equal to 2443.0 MWth. Maximum time step allowed is 0.01s. The denomination time step does not have a real sense here, because the steady-state option uses special numerical methods to reach steady state more rapidly. So, saying that a time step is 0.01s means that the incrementation step is 0.01. This time step was chosen low enough as a larger value brings oscillations that prevent obtaining a good stability of the solution. Steady state was reached after "time" advancement of 194.72, meaning 19472 iterations.

We can verify the initialization of our problem by looking the mass error dm/M. If this is low enough (10^{-4}-10^{-5} or less), then we can trust the results of the steady state run and run some transients. From the output file, we can read that for a total system

mass of 3.306E+5 kg, the mass error (cumulated) is only 13.125 kg, which correspond to a relative error of 3.9E-5, which is acceptable. And in the output file, “err.est” which corresponds to the estimated truncation error fraction at the last advancement is only equal to 2.3099E-08, which is very low. It is possible to adapt the problem to obtain a good initialization level by playing with the friction factors for instance. Because it is a parameter that is not exactly known, we can modify them a little bit from a previous guessing hand calculation so that the problem is well initialized, meaning that the mass error is as low as possible (or at least below an acceptable limit). Figure 2-7 shows the evolution with time advancement of the solution for the steady state calculation. Once we get this, we can start to set up transients.

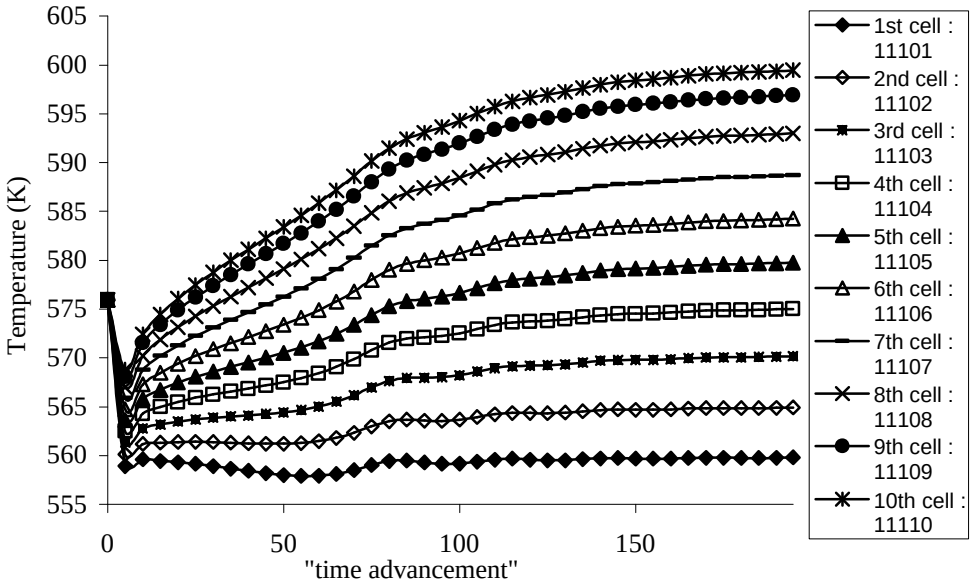

Figure 2-7: Evolution of the temperature distribution during the steady state run.

The purpose of this picture is to show how, starting from the initial conditions (temperatures all equal to 577 °F=575.94 K), a final temperature distribution is reached. The steady state temperature distribution in the core channel is presented in Figure 2-8.

The temperature distribution has an expected behavior. Whereas the central channels have temperatures close to each other's, the outer channel has the lowest temperature and the middle channels are in a kind of intermediate range. And the temperature profile inside a fuel rod is given in Figure 2-9. These shapes may be obtained theoretically. These types of calculation are the major interest of RELAP5. Depending on whether the core model includes cross-flow junctions or not, the steady state conditions obtained are not exactly the same, because coolant is allowed to flow in the transversal direction and is not limited to only axial flow. Coolant flow remains, however, mainly axial. This is treated in the Chapter 3.

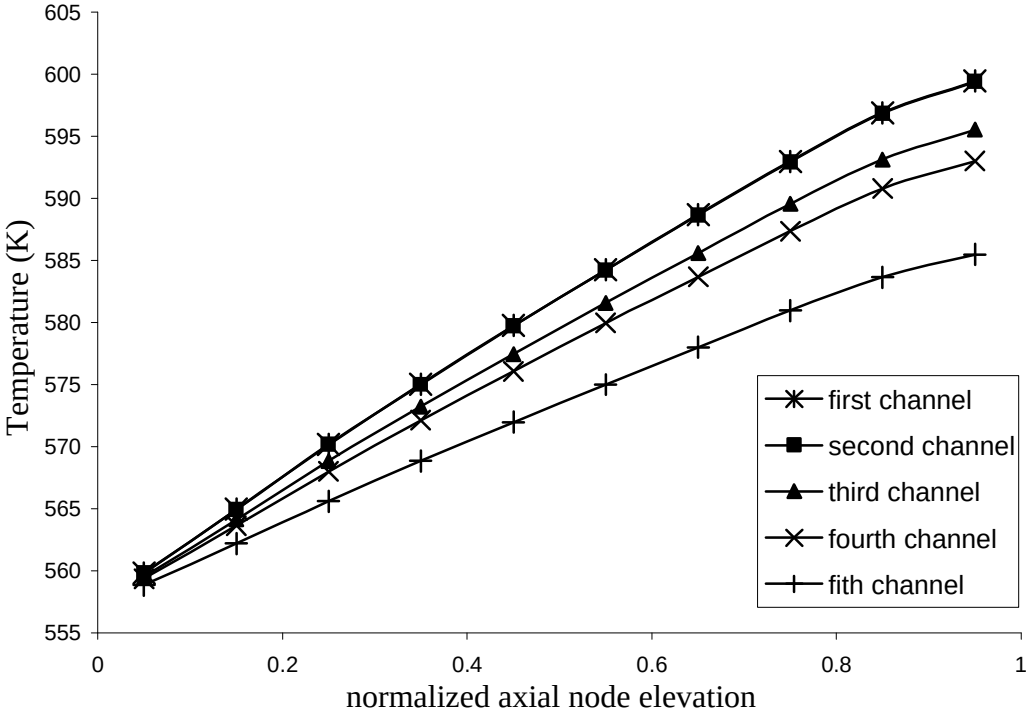

Figure 2-8: Axial coolant temperature distribution the steady state.

The purpose of this chapter was to describe the first tool used in the investigation of the cross-flow calculation. However, results obtained with RELAP5 were not always

convincing, and RELAP5 is not designed to give the level of definition that was needed to achieve a detailed calculation.

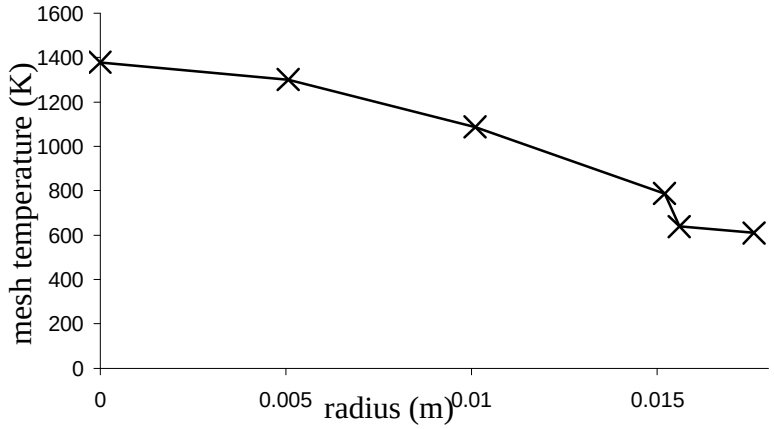

Figure 2-9: Radial fuel temperature profile at the sixth vertical node (height=2.012 m).

Results of the investigation will be discussed in more detail in Chapter 3. Another method was then used to calculate cross-flow occurrence in the core in a more detailed way, by using a Computational Fluid Dynamics (CFD) code. This method, more time consuming may not allow modeling systems as large as RELAP5, but it allows having a precise distribution of fluid velocity in an adapted core model.

CHAPTER 3
PROTOCOL OF EVALUATION OF CROSS-FLOW MODEL USING HIGH RESOLUTION COMPUTATIONAL FLUID DYNAMICS

About FLUENT

RELAP5 is a proven tool for estimating the general properties of a large size system, including all components contained in the reactor loop like pumps for example.

Cross-flow phenomenon in a nuclear reactor core was studied in different ways. The effect of cross-flow can be of a major concern in a case of natural circulation of the coolant in the core. RELAP5 calculates the radial mass flow rates by using a cross-flow junction. The code solves the momentum equation between the two adjacent cells to calculate cross-flow between these two cells. This model in RELAP5 needs to be improved. In order to validate the models used in RELAP5, a similar model was created to calculate cross-flow phenomenon using CFD methods. FLUENT (5) is a code that performs CFD calculations. As the code solves the fundamental conservation equations, results are supposed to be better. It solves the Navier-Stokes equations using a finite element method on a grid that can be generated by the grid generator software GAMBIT. FLUENT4 allows building simple grids with an integrated grid building option. However, another version, FLUENT5, was used as options not available in FLUENT4 were needed, like User Defined Functions (UDF) that can be coded in C. UDF principles will be discussed later in this chapter. GAMBIT was used as an external grid builder, which is feasible as this problem is a simple case. The procedure of grid building with

GAMBIT is explained later on. Boundary conditions have a critical importance in the modelisation of a system and it will be discussed that the major problem in achieving cross-flow evaluation is to setup an adequate model. The boundary conditions available in FLUENT, and those chosen in the model will be detailed in this chapter.

General Overview

Solving the Navier-Stokes equations is a real challenge, as they do not have an exact analytical solution. Thus, numerical tools are necessary to solve numerically the conservation equations. FLUENT is a Computational Fluid Dynamics (CFD) code that solves Navier Stokes equations using finite differences methods. Numerical methods are numerous to solve partial differential equations (PDE), and the one used in FLUENT is described in this chapter. Although discretization of PDE's is powerful, it has important limitations concerning stability of the solution and also from the size of the grid that is chosen. The larger the grid is (or the finer the mesh size is), the more time is needed to solve the problem. Also, the CPU time needed is generally in the order of N^2 for an NxN grid. So, one can not perform calculations for the exact core model as modeling the whole core with all the channels would require too many calculation cells and a quantity of CPU and memory that a computer can not handle. To solve this problem, an equivalent model is used based on a modelisation of the core with different annulus all entered on the centerline of the core. This model will be described in this part too.

The basis idea of using FLUENT is to perform an evaluation of the cross-flow models included in RELAP5. CFD methods, as they calculate the flow patterns and properties at every point of a detailed grid, are more accurate than models used in RELAP. Development of a model requires assumptions to match as well as possible the

actual conditions in the reactor. Also, FLUENT is solving the conservation equations for two dimensions or three dimensions cases. This study will detail the advantage to do a two-dimension run.

Basic Physical Models

For all types of problems, as shown in the user's guide (7), FLUENT solves continuity and momentum conservation equations. If one chooses to include the "energy" option in the setup of the problem, which is required to calculate temperature distributions, heat transfer phenomenon or include compressibility properties, then an additional energy equation for energy conservation is solved. The problem of interest has a cylindrical geometry. Then only a 2D calculation is necessary. There are two types of spaces for this model. The first one is a regular two-dimension space, which calculates on a two-dimension axisymmetric domain. The last one has special properties that will be described later. The conservation equations are written in a regular Cartesian coordinates system for both spaces. For the regular two-dimension domain, the mass conservation equation is written for each phase as follows:

$$\frac{\partial r}{\partial t} + \frac{\partial}{\partial x_i}(r u_i) = S_m$$

The term S_m is the mass source term, which is generally a phase change source term. In the case of a single element, two phase problem, condensation or evaporation of the element is included in this source term.

The momentum conservation equation is written:

$$\frac{\partial}{\partial t}(r u_i) + \frac{\partial}{\partial x_j}(r u_i u_j) = -\frac{\partial P}{\partial x_i} + \frac{\partial t_{ij}}{\partial x_i} + r g_i + F_i,$$

$$\text{and } t_{ij} = \left[m\left(\frac{\partial u_i}{\partial x_j} + \frac{\partial u_j}{\partial x_i} \right) \right] - \frac{2}{3} m \frac{\partial u_l}{\partial x_l} d_{ij}$$

τ_{ij} is the stress tensor and F_i represents the external body forces.

The energy equation solved when needed is:

$$\frac{\partial}{\partial t}(rE) + \frac{\partial}{\partial x_i}\left(u_i(rE + P)\right) = \frac{\partial}{\partial x_i}\left(k_{eff} \frac{\partial T}{\partial x_i} - \sum_{j'} h_{j'} J_{j'} + u_j (t_{ij})_{eff} \right) + S_h$$

k_{eff} is the effective conductivity, $J_{j'}$ is the diffusion flux of species j' and S_h represents any volumetric heat source. This can be a User Defined Function.

It could be useful, in this case, to use a slightly different two-dimension space model to perform our calculations. FLUENT uses a solver in a 2D axisymmetric space. The conservation equations are a bit modified, in which axial and radial coordinates are used (it is still a 2D problem) and axial (u) and radial (v) velocities are calculated. The continuity equation for this coordinates system is written as:

$$\frac{\partial r}{\partial t} + \frac{\partial}{\partial x}(ru) + \frac{\partial}{\partial r}(rv) + \frac{rv}{r} = S_m$$

Momentum conservation equations for axial and radial momentum are more complicated than for a Cartesian mesh:

$$\frac{\partial}{\partial t}(r\,u) + \frac{1}{r}\frac{\partial}{\partial x}(r\,r\,uu) + \frac{1}{r}\frac{\partial}{\partial r}(r\,r\,vu) =$$
$$-\frac{\partial p}{\partial x} + \frac{1}{r}\frac{\partial}{\partial x}\left[r m \left(2\frac{\partial u}{\partial x} - \frac{2}{3}(\nabla \cdot \vec{v}) \right) \right] + \frac{1}{r}\frac{\partial}{\partial r}\left[r m \left(\frac{\partial u}{\partial r} + \frac{\partial v}{\partial x} \right) \right] + F_x$$

and

$$\frac{\partial}{\partial t}(rv) + \frac{1}{r}\frac{\partial}{\partial x}(rruv) + \frac{1}{r}\frac{\partial}{\partial r}(rrvv) =$$
$$-\frac{\partial p}{\partial r} + \frac{1}{r}\frac{\partial}{\partial r}\left[rm\left(2\frac{\partial v}{\partial r} - \frac{2}{3}(\nabla \cdot \vec{v}) \right) \right] + \frac{1}{r}\frac{\partial}{\partial x}\left[rm\left(\frac{\partial v}{\partial x} + \frac{\partial u}{\partial r} \right) \right] - 2m\frac{v}{r^2} + \frac{2}{3}\frac{m}{r}(\nabla \cdot \vec{v}) + r\frac{w^2}{r} + F_r$$

w is the swirl velocity.

Numerical Solvers

This part will present numerical solvers available in FLUENT. Different algorithms can be used, depending on the type of problem that needs to be solved. Also, boundary conditions are to be chosen among the list of available models presented in this part. All types of boundary conditions are not always compatible with each other, or even with the type of problem, depending on the geometry or the flow conditions for example.

Numerical schemes and discretization

There are two different numerical schemes in FLUENT, the so-called "segregated" solver and "coupled" solver. The principle of both solvers is to solve the integral form of the equations of conservation of mass, momentum and energy over a mesh grid. Turbulence related equations (like in the k-ε model) also employ these solvers. A detailed description of both methods can be found in the FLUENT user manual (8). This paper focuses mainly on the segregated solver.

Both solvers use a control volume technique. For this method, the domain is divided in control volumes delimited by a computational grid. The grid choice depends on the geometry, the type of problem to be solved (heat transfer, fluid flow), and the resolution needed for the solution. One may choose simple orthogonal grid for simple geometry where more resolution in certain regions of the domain is not needed. However, if the focus is on boundary layers or some regions around obstacles, then one may need to use a finer mesh grid in the interesting regions of the domain. The generation of this type of grid may be very time consuming, and can need specific tools. The software GAMBIT was used to generate a grid for two reasons. First, it is a convenient and user-friendly grid generation software. Second, the version FLUENT5 does not generate grids by itself.

The governing equations, which are actually partial differential equations, are integrated over a control volume to obtain a set of algebraic equations involving all variables. These equations are then linearized and the system obtained is solved. These two steps (linearization and resolution) are different depending on the solver.

In the segregated solution method, starting from an initial estimation or the current solution, the fluid properties are updated. Next, the momentum equations for every direction are solved using current values for pressure and face mass fluxes, in order to update the velocity field. A Poisson type equation obtained from mass conservation and linearized momentum equation is solved to correct pressure and velocity field so that mass conservation is satisfied. When needed, scalar quantities like energy or turbulence are calculated (by solving appropriate equations). The last step is to check the convergence, which is tested on the residual of the unknown parameters. The convergence level of each residual can be chosen separately. In the segregated solution method, terms are treated explicitly and implicitly with respect to the iteration advancement variable. The variable treated implicitly is the equation's dependent variable. Thus, for each variable, we have a set of linear equations, one for each cell in the domain. The principle of the segregated solver is that it solves a system of equations for the variables one after the other.

Different discretization schemes are available for each governing equation. As noted earlier, the code uses a control-volume technique. The governing equations are integrated over the volume of the cell, such that the values of pressure and velocity are needed at the cell faces. However, FLUENT uses a co-located scheme, meaning that both pressure and velocity are stored at the center of the cell. Therefore, an interpolation

scheme is needed for pressure and velocity. Different schemes are available in FLUENT. This study used the standard scheme for pressure described in reference (6). The momentum interpolation utilizes a first order upwind scheme. It is assumed that the variable face value is equal to the cell center value of the variable in the upstream cell. As observed, the second step, after solving the momentum equations, is to perform a pressure and velocity field correction. The pressure velocity coupling is realized with the SIMPLE algorithm. This algorithm provides a pressure correction and is described in the FLUENT user's guide (8). Since the energy equation must be solved, interpolation for energy is done using a first order upwind scheme. This is also the case for k and ε transport equations. More extensive descriptions of numerical methods employed by FLUENT can be found in the FLUENT user's guide (8).

Boundary conditions

In computational fluid dynamics, conservation equations govern the state of the fluid and its behavior inside the computation domain. The state of the fluid at the boundaries has to be well known to adapt the solution to the specific case to be solved. The choice of boundary conditions and additional models will be decisive in the matching of the FLUENT model to RELAP5 model. Basically, we need to have boundary conditions for the outer walls, the inlet and the outlet regions of our domain. FLUENT permits many different boundary condition (BC) types (9). A short description of the most commonly used and those used for this model will follow. All the following parameters can be fixed as constant or defined by a User Defined Function (UDF), or simple piecewise linear distribution.

The inlet BC can be modeled using the following models:

The mass-flow inlet type BC. One can choose the inlet mass flux (kg/s) or mass flow rate (kg/m2.s) for the chosen surface. One is also asked to define the inlet fluid temperature and pressure. One should also provide the flow direction. It is possible by writing the two components of the flow as work in two dimensions.

The pressure inlet type BC. One may choose the initial gauge pressure of the fluid when it enters the calculation domain, also one need to provide the inlet temperature and the turbulence model chosen.

The velocity inlet type BC. For a specified direction, one can choose the velocity vector components, and the temperature of the inlet fluid. The turbulence model needs again to be entered.

The outlet boundary conditions can be chosen among the following types:

The outflow type BC. One may simply choose the fraction of fluid that leaves through this surface by choosing the flow rate weighting. This type of boundary condition requires a fully developed flow.

The pressure outlet type BC. One needs to input the gauge pressure at the outer surface and the temperature of the backflow with the turbulence model. The advantage on the outflow boundary condition is that the flow does not need to be stabilized to have this type of boundary condition.

These are basically the two interesting models of BC for the outlets. The walls have specific types of BC that can be personalized to every kind of problem. As one choose to solve the energy equation, one may impose boundary conditions that involve temperature and heat flux characteristics.

The wall type BC. It can be largely personalized by choosing the type of thermal boundary condition: it can be set by heat flux, temperature, convection, radiation or mixed type of boundary conditions. For every kind of temperature, one will need to enter the wall thickness and the heat generation rate, and also whether the temperature or the heat flux at the surface or the heat transfer coefficient or the emissivity of the wall and the temperature of emissivity. A mixed type BC will associate convection and radiative heat transfer boundary conditions. Also in every case the user needs to input the wall roughness and the material name. Parameters like heat flux, temperature, heat transfer coefficient or emissivity can be modeled with a constant parameter or by using a UDF.

The symmetry type BC. If one chooses to have this type of boundary condition, the normal velocity is equal to zero at the symmetry plane and normal gradients of all variables are set to zero. This has to be used for a geometry that is actually symmetric, or it can also be used to model “slip” walls, without shear stress.

The “axis” type BC. For an axisymmetric problem the physical value of a particular variable at a point on the axis is determined by using the cell value in the adjacent cell. For an axisymmetric geometry, the user should employ an “axis” boundary condition type rather than the “symmetry” one.

The interior of the domain can be chosen as solid or liquid. In all these cases, the liquid type of interior fluid is considered. Any kind of boundary condition can be imposed at the limits, but this choice has to be coherent.

User defined functions

User defined functions (UDF) can be used to specify very detailed distributions of boundary variables, source terms, property definitions, wall heat flux or solution

initialization. The UDF have to first be coded in the C language. The UDF is then compiled by FLUENT (for the most basic utilization) and then information contained in the UDF is incorporated in the FLUENT model to enhance the capabilities of the code. In these tests, UDF were used to model a power source in the reactor, and inlet velocity distribution, which is not elementary distributed. This type of function could also be used to model the temperature dependence of the water density. As temperature varies slightly, the density is expected to change only a few percent, which will have a negligible effect. Power density is different in the channels of the core, due to the difference in peaking factors. UDF can also be useful to set up a specific inlet velocity profile. In RELAP5, the inlet velocity is the velocity averaged at the junction. However, for this model, a profile following the $1/7^{th}$ power law at the wall boundary can be proposed as an alternative for inlet velocity profile. A UDF is used for this modelisation. The description of all possible user defined functions can be found in the FLUENT user guide (9) and (10).

Turbulence Modeling in FLUENT

In this study, the flow is turbulent, as Reynolds number is very high (about 10^5-10^6). Reynolds number is equal to $\mathrm{Re} = \frac{\rho v D_h}{\mu}$ where D_h is the hydraulic diameter, ρ is the fluid density, v is the fluid velocity and μ is the fluid viscosity. As there is a quite high temperature fluid, viscosity is really low, which makes the Reynolds number high. Also, there is a large diameter system and treating the problem like a laminar flow would not make any sense. A turbulent viscosity term has to be taken into account, as seen in the previous part. The way this parameter is calculated depends on the turbulence model one chooses. Unfortunately, there is no single universal model for turbulence modeling.

Actually, turbulence modeling may need to be developed for each specific case, as it depends a lot on the fluid type and properties, and on the geometry. Turbulent flows are characterized by fluctuating velocity fields. As these fluctuations are of very small scale or high frequency, it is difficult and too expensive to simulate them from an engineering point of view. Governing equations can be averaged over time or ensemble so that resulting modified equations are much easier to solve. But then, models are needed to determine additional unknown variables. Turbulent viscosity can be calculated with different methods that can require more or less parameters of the flow, like turbulent kinetic energy k, or even the dissipation rate of the turbulent kinetic energy e .

The velocity field (and any scalar quantity field) can be decomposed in two distinct components (mean and perturbation) such as:

$$u_i = \bar{u}_i + u'_i$$

The turbulent kinetic energy is defined as $k = \frac{1}{2}\left(\overline{v_1'^2} + \overline{v_2'^2} + \overline{v_3'^2}\right)$, using the perturbation terms. As the average of the perturbation term is zero and as one takes a time-averaged form of the continuity and momentum equation, one obtains, for the mean velocity, written u_i now:

$$\frac{\partial r}{\partial t} + \frac{\partial}{\partial x_i}\left(r u_i\right) = 0$$

$$r\frac{Du_i}{Dt} = -\frac{\partial p}{\partial x_i} + \frac{\partial}{\partial x_j}\left[m\left(\frac{\partial u_i}{\partial x_j} + \frac{\partial u_j}{\partial x_i} - \frac{2}{3}d_{ij}\frac{\partial u_l}{\partial x_l}\right)\right] + \frac{\partial}{\partial x_j}\left(-r\overline{u'_i u'_j}\right)$$

These are the “Averaged Navier Stokes Equations”. d_{ij} is the Kronecker symbol. The second term in the right hand side of the equation represents the divergence of the viscous constraints tensor. The effects of turbulence appear in the Reynolds stress term

$t'_{ij} = -r\,\overline{u'_i\,u'_j}$ that requires a specific modeling to close the Reynolds averaged momentum equation. In analogy to the viscous stress term in laminar flows, the turbulent stress term has been proposed to be proportional to the mean-velocity gradients. This concept has been proposed by Boussinesq in 1877, and has been used as a basic to numerous turbulence models. The Boussinesq eddy viscosity hypothesis for the divergence of the Reynolds constraints tensor is written as:

$$-r\,\overline{u'_i\,u'_j} = m_t\left(\frac{\partial u_i}{\partial x_j}+\frac{\partial u_j}{\partial x_i}\right)-\frac{2}{3}\,rkd_{ij}$$

The term μ_t is called turbulent viscosity and has to be determined to be able to evaluate the Reynolds stress. Contrary to the molecular viscosity μ, μ_t is not a fluid property but depends strongly on the state of turbulence. So μ_t may vary greatly from one point to another in the fluid, especially close to the boundaries, as in walls for instance. Many models have been developed to calculate turbulent viscosity. Some of them are very simple and based on empirical correlations, but other models are more complex and mix theoretical and empirical considerations to setup transport equations for turbulence-related quantities used to obtain the turbulent viscosity. So the Boussinesq eddy viscosity hypothesis does not constitute the whole turbulence model, but it provides the framework for constructing a real model. The main problem is actually to determine the distribution of μ_t. A comprehensive review of turbulence models and their application in hydraulics is presented in reference (12) and (13).

An algebraic model may be sufficient for this simulation, as there is a very simple geometry. The principle of an algebraic model is to determine the turbulent viscosity only by one single relation. The most common zero-equation model is also called Prandtl

mixing-length model. A characteristic length of the turbulence is introduced: the Prandtl mixing length. This is basically the length along which an eddy remains identical mechanically. The turbulent viscosity is then calculated as:

$$u_t = l_m^2 \frac{\partial \overline{U}}{\partial y}$$

$\overline{U}$ is the mean velocity gradient along the transversal direction. l_m is the mixing length. The calculation of l_m is then the problem. A satisfactory estimation for l_m is illustrated in Figure 3-1. The parameter d is defined as the layer width. It is calculated as the distance from the wall to the 1% point of the outer edge, or the point where velocity differs by 1% from the free stream velocity. The constant k is the Von Karman constant and is equal to k =0.41. l is equal to l =0.09. These constants have been determined originally by Patankar and Spalding (14).

For developed duct flows (channels, pipes), the mixing-length distribution is well described by Nikuradse's formula (15):

$l_m/R = 0.14-0.08(1-y/R)^2-0.06(1-y/R)^4$

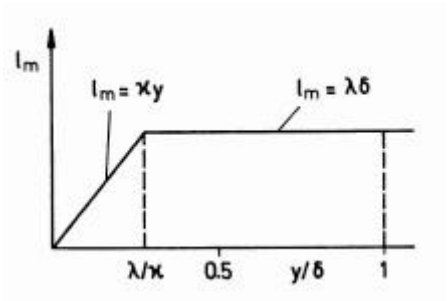

Figure 3-1: Mixing-length distribution in wall boundary layers.

However, this is a very approximate modelisation, and as a high intensity cross-flow phenomenon is not expected, one may want to have a better model to treat turbulence so that the order of magnitude of the error introduced by the turbulence

treatment would not affect the results of cross-flow calculation. Furthermore, such a zero equation model is not available in FLUENT.

Six models of turbulence can be used in FLUENT, each of them being adapted to a certain type of situation. They are: Spalart-Allmaras model, k-e model (Standard (16), RNG (17) and Realizable (18)), Reynolds stress model and Large Eddy simulation. Two-equation models are the most widely used in engineering simulations. This study will use k-e models, which are respectively one-equation and two-equation models and use a Boussinesq eddy viscosity hypothesis for the divergence of the Reynolds constraints tensor. Spalart-Allmaras model could also be used without any problem

One-equation Spalart-Allmaras model

Although this model has been originally developed for aerospace flows involving wall bounded flows, it has been adapted to fit with the needs of FLUENT and high Reynolds number calculations. However, as this model is quite new, results in some very specific cases should be evaluated with caution. This is a simple one-equation model that uses the Boussinesq hypothesis. The main advantage of this method is that one does not need to calculate a length scale related to the local shear layer thickness. The unknown of the transport equation solved in the Spalart-Allmaras model is a modified form of the turbulent kinematic viscosity. Constants used in the model are these proposed by default in the code. A detailed description of the Spalart-Allmaras model is done in the FLUENT user manual (7) and in the original paper (19).

Two-equation k-epsilon model.

This k-e model is used as a better alternative to the one-equation Spalart-Allmaras model. This is a very common turbulence model as it is based on semi-

empirical considerations. Since it was proposed by Launder (16), the k-e model has always been used and improved. In this model, the transport equations of turbulent kinetic energy (k) and its dissipation rate (e) are solved. Basically, the transport equations of k and ε are built on the classical balance equation:

Rate of change + Convection = Diffusion + (generation – destruction)

The transport equations for the Standard k-ε model are:

$$r\frac{Dk}{Dt}=\frac{\partial}{\partial x_i}\left[\left(m+\frac{m_t}{s_k}\right)\frac{\partial k}{\partial x_i}\right]+G_k+G_b-re-Y_M$$

where G_k is the production of turbulent kinetic energy defined as $G_k=-r\overline{u'_i u'_j}\frac{\partial u_j}{\partial u_i}$, determined using Boussinesq assumption, G_b is the generation term due to buoyancy, defined as $G_b=bg_i\frac{m_t}{\mathrm{Pr}_t}\frac{\partial T}{\partial x_i}$. Y_M is the dilatation dissipation term for high Mach number flows, not relevant here. s_k is the turbulent Prandtl number for k.

$$r\frac{De}{Dt}=\frac{\partial}{\partial x_i}\left[\left(m+\frac{m_t}{s_e}\right)\frac{\partial e}{\partial x_i}\right]+C_{1e}\frac{e}{k}\left(G_k+C_{3e}G_b\right)-C_{2e}r\frac{e^2}{k}$$

where C_{1e}, C_{2e} and C_{3e} are constants, s_e is the turbulent Prandtl number for e. In FLUENT, constants have the default values C_{1e}=1.44, C_{2e}=1.92 C_{3e}=0.09, s_k=1.0 and s_e=1.3. These values have been determined experimentally. However, the user can change them in FLUENT. This study used only the Standard k-e model without changing the default constants. A detailed description of other two-equation models can be found in the user manual (7).

In this model, the turbulent viscosity is computed as $\mu_t=\rho C_\mu k^2/\varepsilon$. This value can then be used to calculate the Reynolds stress, from the Boussinesq assumption. The main difficulty is to choose the boundary conditions for k and e. The user guide manual proposed the following approximations to evaluate the initial conditions for k and e.

- The turbulent kinetic energy k (m^2/s^2) can be estimated from the turbulence intensity I defined as $I = \frac{u'}{u_{avg}} \cong 0.16\left(\mathrm{Re}_{D_H}\right)^{-1/8}$: $k = \frac{3}{2}\left(u_{avg} I\right)^2$
- The turbulent dissipation rate e (m^2/s^3) can be estimated from a length scale $l = 0.07 D_H$. Then e is approximately equal to $e = C_m^{3/4} \frac{k^{3/2}}{l}$. The constant Cμ has been determined equal to 0.09.

This research used these methods to determine our inlet boundary values for k and e.

Defining a CFD Method for Evaluating RELAP5 Cross-Flow Model

RELAP5 uses a coarse integral method to solve the conservation equations. The cross-flow model is very simplified, as presented in the Chapter 2. A protocol has been developed to determine an evaluation of this model. A very simple system has been studied with cross-flow calculations. This part presents the two different models used to perform the simulation with FLUENT and RELAP5. The system consists in a simple vertical pipe where the fluid (liquid water) is moving upwards. Conditions of operation are these of a real reactor. Inlet fluid temperature is 555 K, and the pressure is 15.68 MPa. The inlet conditions are very specific. This study used a velocity profile distribution to analyze the impact of velocity distribution for cross-flow calculation, as velocity is a

parameter that cause cross-flow. Figure 3-2 represents the system that has been calculated with FLUENT and RELAP5. Also, it is possible to have internal heat generation in the models to study the effect of temperature on the cross-flow occurrence. The velocity profile is radius dependent, with the central part of the flow at a higher velocity.

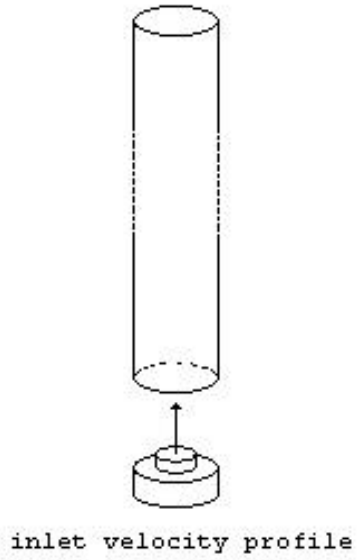

Figure 3-2: Basic geometry studied with RELAP5 and FLUENT.

FLUENT Model

The FLUENT model is supposed to be as close as possible to the real geometry and operating conditions. Figure 3-3 shows the calculation domain representing the pipe of the Figure 3-2.

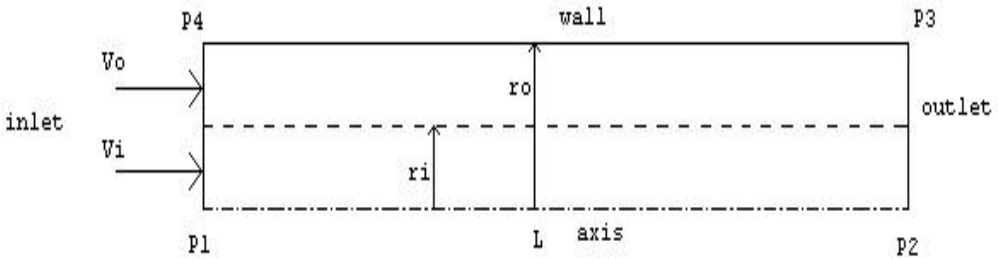

Figure 3-3: FLUENT calculation domain of the system.

Calculations were performed on a two dimensional axisymmetric space, as boundary conditions were applied with a cylindrical geometry. The distance r_i does not represent an actual boundary, but it is used as a limit to impose internal heat generation, and also it will serve as a basis to define velocity profiles. Also, this is the limit that has been used to build the RELAP5 equivalent model, where the channel was divided in two pipes linked together with the cross-flow junction of interest. The calculations were performed on this simple surface, so a grid was generated for this domain. The software GAMBIT was used.

GAMBIT grid generation

Grid generation is a very important step in CFD problems. Generally, grid generation represents a large fraction of the total CPU time necessary to the resolution of a problem. If the geometry of the domain is complex, it can take a long time to build an adequate grid. This study used a very simple geometry. Since the calculation domain is a rectangular area, an orthogonal grid was used. The GAMBIT software generated the grid, as this task cannot be handled by FLUENT5 (contrary to FLUENT4 that allowed building simple grids). Following is a description of the few steps necessary for grid construction and the establishment of some reference points.

The first step is to set the limit points that will be used to create the edges. GAMBIT allows creating the points with their coordinates.

The next step is to create the edges in the domain. In the present case, the edges are the external limits of the domain. So edges are created for both walls and open boundaries. On Figure 3-3, the four edges are created with the four points P1, P2, P3, and P4. They correspond to the inlet zones, one outlet area, and the two side boundaries,

corresponding to the surrounding wall and the centerline of the physical domain that is modeled by a real boundary. Once edges are created, it is possible to create faces and to build volumes. This option was not needed in the 2-D problem.

The next step can be very time consuming in term of CPU time. However, for this simple domain, the grid generation is very fast. For an orthogonal grid, the first step is to generate the mesh edges. For every edge, a one-dimensional mesh is generated, each cell having the same length. It could be possible to create a finer grid at the boundary layer if the purpose of the study was to have detailed description of the events occurring close to the wall surfaces. Finally, the last step is to create the final mesh of the domain. In GAMBIT, the "mesh faces" option generates the final mesh, based on the mesh edges. Then, after assigning specific boundary types to the boundaries, it is possible to export the grid to FLUENT, where materials properties and boundary conditions are specified.

Boundary and operating conditions

The boundary conditions are very important, and will be the determinant in the validity of the model. As a commercial code is used that is reliable and uses powerful numerical methods, the only way one can adapt the solver to a problem is by setting good and adapted boundary conditions. The inlet and outlet boundary conditions will especially have a capital effect on the behavior of the fluid in the calculation domain.

Operating conditions. The operating conditions need also to be specified before beginning the calculations. The reference for the pressure is at the outlet of the rectangular calculation model, on the centerline. Also, an option can be activated to take into account the effect of gravity by setting the acceleration of gravity (9.8 m/s^2) and also

the direction to which it applies (vertical top to bottom). Operating pressure was chosen equal to 15.68 MPa.

Outlet boundary. The outlet was set as an outlet pressure boundary with a static gauge pressure equal to zero (which means that the absolute outlet pressure is the operating pressure). An outflow could not be used, as it requires the flow to be fully developed.

Wall boundaries. The centerline boundary was represented by an axis type boundary condition. The outer wall ("wall" on Figure 3-3) was of a wall type. An adiabatic wall was chosen for the outer boundary (meaning heat flux set to zero). Choice of wall roughness will determine the losses due to friction on the wall and of course have a strong effect on the velocity profile (at least on the transversal direction) for a domain with a mall radius, where the wall boundary layer can be visible. A roughness height (k_S) equal to 10^{-4}, and a roughness constant approximately equal to 0.5 are acceptable numbers.

Inlet boundary. The inlet boundary was set to have the velocity fixed by an inlet velocity type BC. As velocity inlet boundary conditions was set, other parameters like turbulence terms boundary values need to be specified.

Fluid properties. As one considers an incompressible flow, the material properties are almost constant values. However, water properties tables (20) were used to set the water properties respect to temperature as a piecewise linear function. This has an effect only when heat is added to the fluid:

Two different domains were studied. The first one represents a large pipe, where the wall effects were avoided because of the large diameter. The second one is a much

smaller one. Based on the geometry shown Figure 3-3, two models were built. The first one had an outer radius of 0.4 m, and the pipe was divided into two sub channels such that r_i=0.2m and r_o=0.4m. The length of the pipe L was equal to 5.0m. The second model was a much smaller one. The dimensions of the pipes were r_i=0.5cm, r_o=1.0cm and the length of the pipe was taken 20 cm. Results of calculations on these two models are presented in the Chapter 4.

RELAP5 Equivalent Model

An equivalent model was built for the analysis of the cross-flow phenomenon inside the pipe. For this, the pipe was divided axially into two pipes. The Figure 3-4 shows the nodalization diagram of the equivalent system. Pipes, which area is the same as the area of the two sub channels that compose the pipe Figure 3-3, represent the two axial channels. This means that the cross section area of the pipe 100 is equal to $p\ r_i^2$. The area of the pipe 110 is then equal to $p\ (r_o^2-r_i^2)$. Volumes 88, 98, 130 and 131 are time dependent volumes and represent reservoirs to provide the water flow in the system. Pressure in 130 and 131 set the pressure in the system. Pressure has then to be adjusted in volumes 88 and 98, where the temperature of the entering fluid is set. Time dependent junctions 89 and 99 regulate the inlet velocity for the system. The junctions 120 and 121 are simple single junctions. The set of Junctions 112XX is a multiple cross-flow junction that allows the fluid going from a channel to the other. This is the junction of interest in this study. The pressure in the two top Volumes 130 and 131 is set to 15.68 MPa and is not changed. Only the pressure in the inlet time dependent volumes is adapted to each problem. The temperature in the inlet Time Dependent Volumes 88 and 98 is set to 555 K.

The inlet velocity regulated by the time dependent junctions 89 and 99 is the parameter that sets the flow in the system, and is specified for each test in the Chapter 4. The cross-flow junction area in the RELAP5 model has been set as the outer area of the cylinder of radius r_i and height equal to the height of a nodalization cell. Heat structures are used to provide heat to the system and are attached to the volumes 110 and 100. An additional heat structure is added to realize heat conduction between channels 1 and 2. A copy of the RELAP5 input deck is provided in Appendix C.

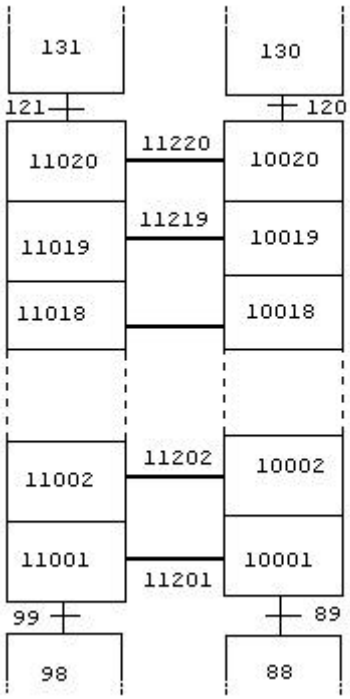

Figure 3-4: Nodalization diagram of the equivalent RELAP5 model.,

The results of the equivalent simulations with FLUENT and RELAP5 are presented in Chapter 4.

CHAPTER 4
CROSS-FLOW CHARACTERIZATION AND EVALUATION OF RELAP5 MODEL

This chapter will present the results from different simulations with FLUENT and RELAP5. For each case, cross-flow has been calculated. First, RELAP5 has been run for a steady state case and a power surge transient to characterize cross-flow phenomenon in a real case simulation. And then, the attention is focused on the cross-flow phenomenon itself by using the two models described in Chapter 3.

Surry Reactor Calculation for a Steady State and a Simulated Power Surge Transient

Cross-flow is predicted in both the steady state and transient cases. The results will show that the impact of taking into account cross-flow in the core is real.

Steady State

In the case of a steady state calculation, no attention is focused on the evolution of the different variables during the calculation phase. Those values have indeed no physical meaning, since the code uses numerical tricks to reach steady state more rapidly, and then the iteration step size does not correspond to a real time value. By looking at the mass flow in the axial channels, different results can be observed whether cross-flow is considered or not. Without cross-flow junction, the mass flow is constant along the core length (due to mass conservation). Though, velocity is increasing as temperature increases and density decreases. The relative mass error introduced by numerical

calculations along the channel is less than 10^{-4} for a core without cross-flow. Table 4-1 shows the axial mass flow in the five hot core channels for the case of a purely axial core or a core with cross-flow junctions between the axial channels.

Table 4-1: Comparison of axial junction mass flow for a core with and without cross-flow.

	Axial mass flow (kg/s) for core with cross-flow				
junction# \ channel	1	2	3	4	5
inlet	387.24	1549.0	2788.2	4647.0	2788.2
1	387.09	1548.4	2788.2	4648.0	2787.8
2	386.76	1547.1	2787.6	4648.9	2789.2
3	386.51	1546.1	2787.2	4649.9	2789.9
4	386.3	1545.2	2786.8	4650.3	2790.9
5	386.02	1544.2	2786.4	4650.9	2792.1
6	385.79	1543.2	2785.7	4651.1	2793.8
7	385.74	1543.1	2786.2	4651.8	2792.9
8	385.22	1540.9	2784.8	4653.3	2795.5
9	385.51	1542.3	2785.4	4650.4	2796.2
outlet	383.8	1535.4	2784.4	4662.1	2794.2
	Axial mass flow (kg/s) for core without cross-flow				
actual data	382.26	1529.1	2762.8	4615.1	2768.2
normalized data	385.49	1542.00	2786.11	4654.04	2791.56

For a more accurate comparison, data have been normalized to a same total core mass flow. The mass flow rate for a closed-channels core is close to the one at the different axial junctions along the core allowing cross-flow, but still a difference is noticeable. For a given channel, the closed-channel value is roughly an average value of the axial mass flow in the open channel case. The difference comes from the cross-flow consideration. However, as can be seen on Figure 4-1, in the steady state conditions, cross-flow is much smaller than the main axial mass flow, which is expected. This figure

shows the magnitude of cross-flow between the five different channels that compose the core. The sign of the calculated cross-flow represents its direction. The way the channels are numbered in the RELAP5 inputs, a positive value for cross-flow means that the flow is going outwards. The total cross mass flow is only about 0.5% of the total axial mass flow. This is due to the fact that the pumps drive the flow axially.

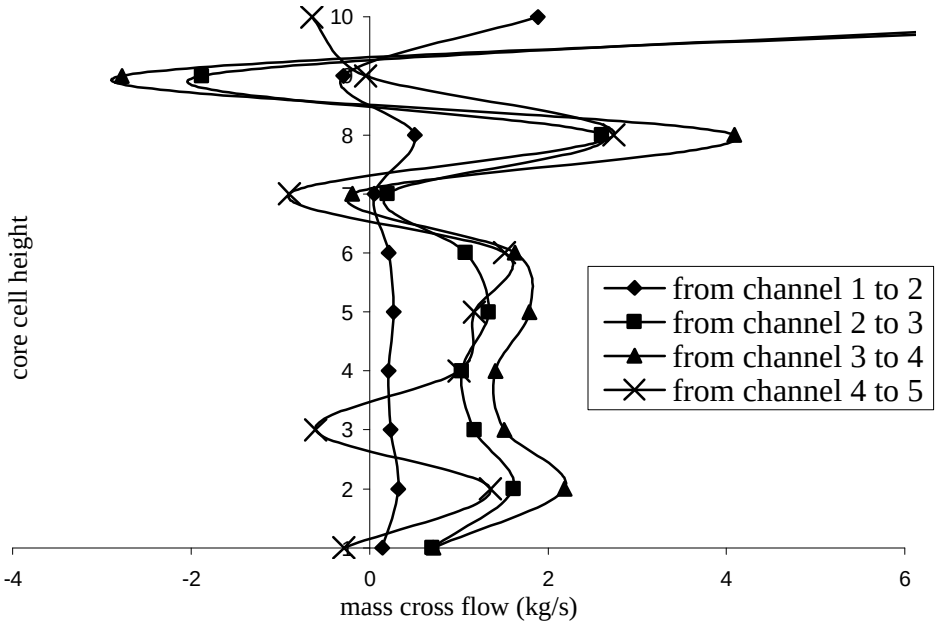

Figure 4-1: Cross-flow magnitude versus height in the core for a total power of 2443MW.

However, to have a better idea of the relative importance of cross-flow from a junction to the other, it is better to look at the mass flux at the junctions. Figure 4.2 shows mass flux for cross-flow versus cell height in the core. This one is calculated by dividing the mass flow by the cross-flow junction area. Actually, the direction of the cross-flow is more interesting. According to the sign of the mass flow, and looking at the setup of the junctions, there is a cross-flow going outwards for all central channels. The outer junction

is a little bit different. This kind of prediction is surprising as different parameters can be considered:

- Temperature: the temperature is higher in the central part of the core, which should, by density difference, push the flow inwards.
- Axial velocity: the axial velocity is changing along the core, but always the axial velocity in the central parts of the core is higher than at the periphery, which means that the pressure difference induced by velocity differences should also drive the flow inwards.

If the conditions are not constant anymore, and if a transient phase is taken into account where conditions are changing in the core, then cross-flow will be different.

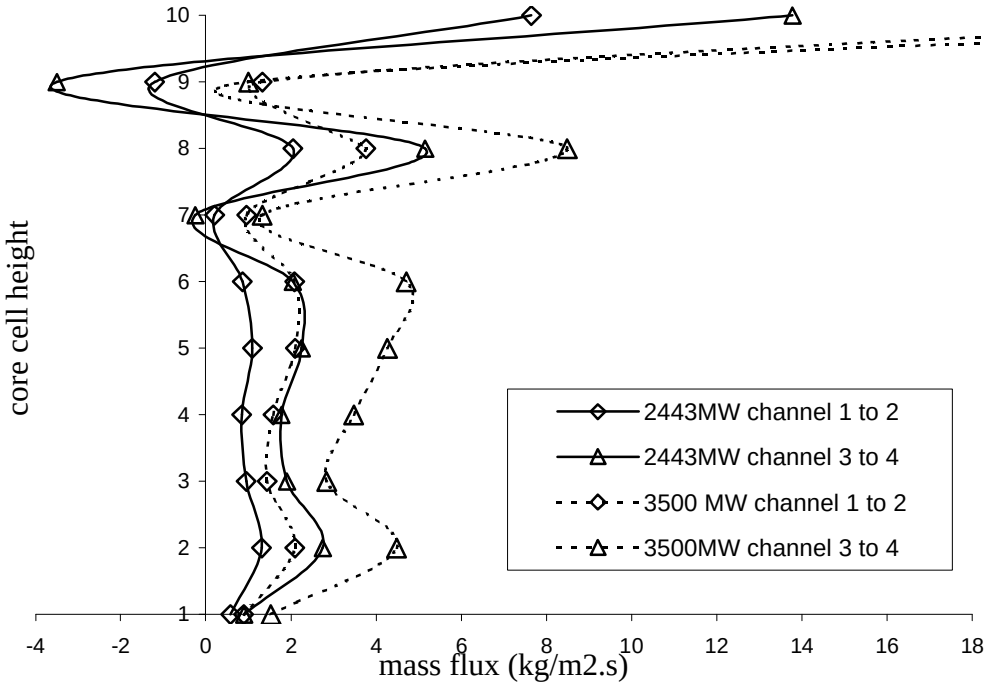

Figure 4-2: Cross-flow mass flux versus core cell height.

Now different power levels can be considered. RELAP5 will predict different cross-flow magnitudes for different power levels. As the mass flow is set constant in the

system, only the temperature of the fluid has an effect on the phenomenon. For different power levels, the steady state cross-flow value was calculated, and normalized to the inlet mass flow in the reactor. Figure 4-3 shows that in a general manner, cross-flow magnitude is increasing when power is higher.

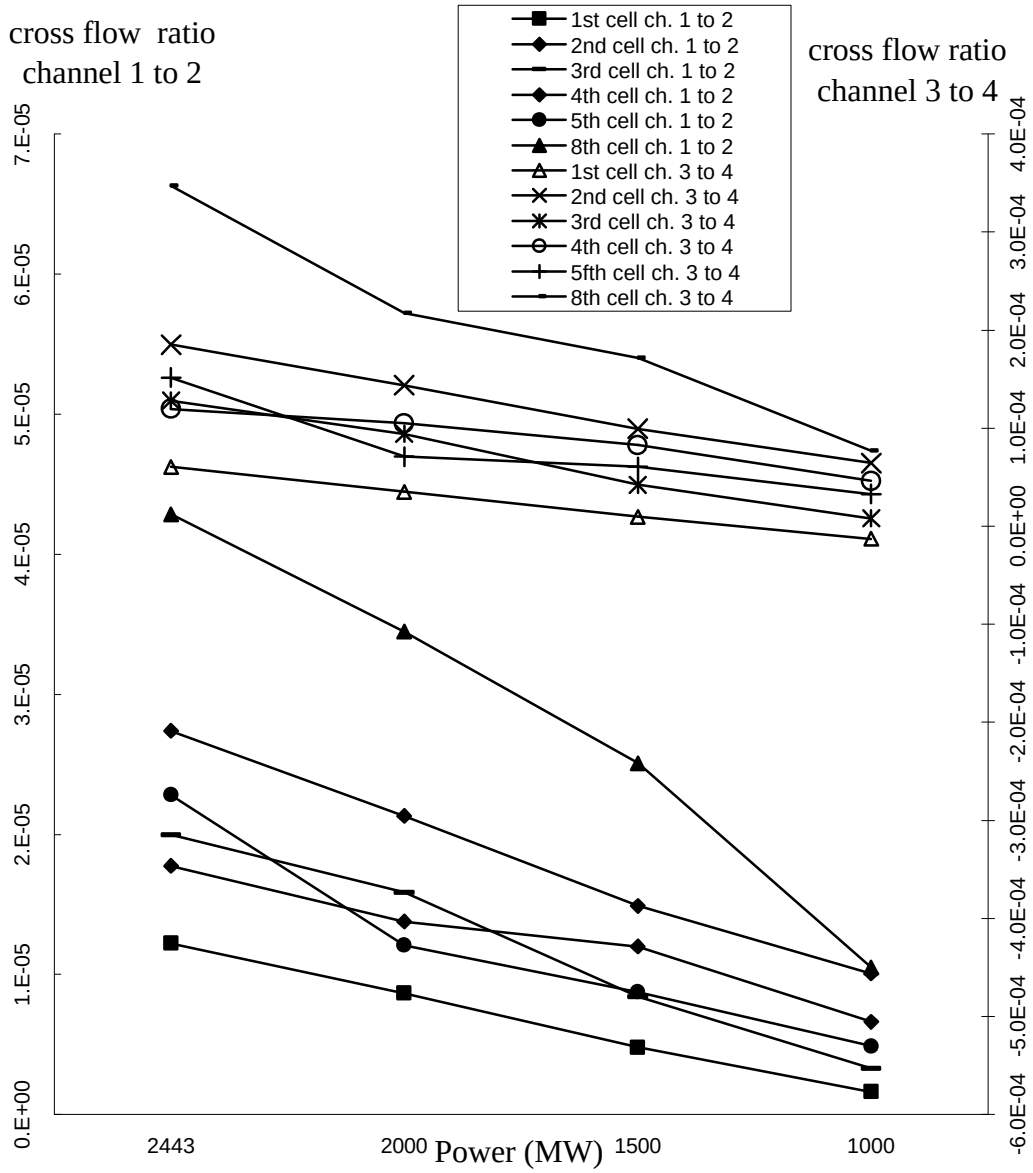

Figure 4-3: Ratio of cross-flow to axial flow for different power levels and for different height in the core.

This figure represents the ratio of the fluid flow in the radial direction to the bottom flow in the axial direction. These four cases represent steady state runs. The cross-flow is noticeable very low. However, a good point to remember is that the mass flow in the loop is maintained constant, and then for each case, there is approximately the same mass flow in the core. Therefore, cross-flow cannot be mainly caused by mass flow. The parameters that can make the flow go radially would be the density difference, since the temperature profile in the core is not flat, lowering the density in the central part where flow temperature is higher. Indeed, looking at the level of the fifth cell (Hydrodynamic Volume 11105, etc…) reveals a difference of temperature between the center channel and the outer channel of about 1%. This makes a very small difference. Density variation is also small. But added to this phenomenon, axial velocity is higher at the center of the core than at the periphery.

Transient Case: Simulation of a Power Surge Transient

The transient case being considered consists in a power surge transient. RELAP5 allows using two methods to input power in the core. One is the reactor kinetics calculation. But as the interest resides in the thermalhydraulic behavior of the core, the other method using a power table and setting the total power in the core was preferred. The use of the power fraction factors in the heat structures does the repartition of the power in the different channels. The power transient is represented in Figure 4-4. The reactor model is built to keep a constant mass flow rate in the reactor equal to 4100.0 kg/s in each leg. Then, as the inlet mass flow in the core remains constant, the impact of the power level on a steady state can be observed, and also during the transient phase, as

temperature increases and physical properties are consequently modified (much more than during the temperature change across the core).

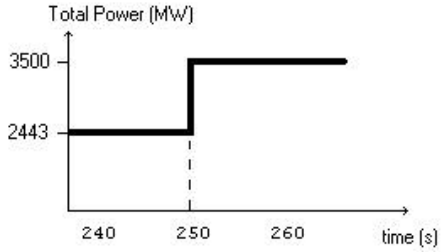

Figure 4-4: Power transient simulated in the transient test.

The calculations were done using the restart option of RELAP5, starting from the steady state determined in the previous part. The general conclusion that can be made after analysis of the results of this investigation is that the power level in the reactor has an effect on cross-flow magnitude. As mass flow in the core is constant, fluid temperature increases when increasing power in the reactor.

Cross-flow magnitude is larger for a greater power level. As can be seen in Figure 4-5, and also as in the previous part in Figure 4-3, the mass flux through the cross-flow junctions is larger when power is larger (whatever the sign of the cross-flow is).

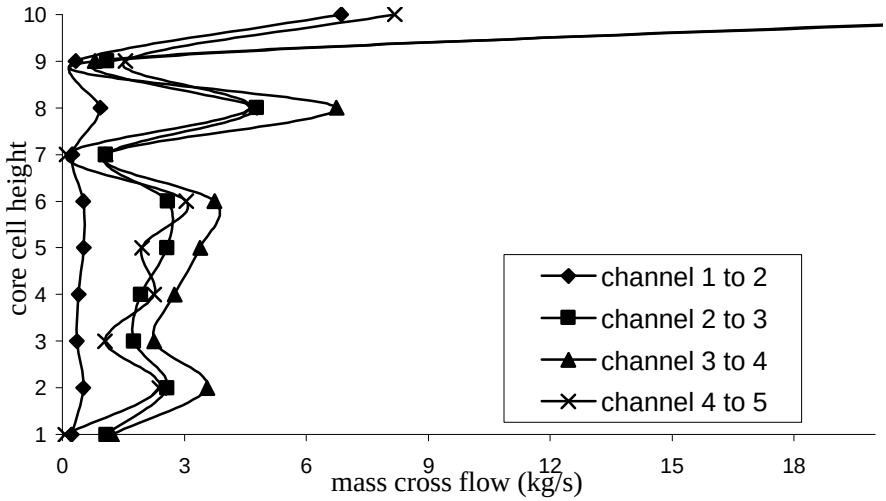

Figure 4-5: Cross-flow magnitude versus height in the core for a total power of 3500MW.

To illustrate the transient phase of the cross-flow, focus will be drawn on the central channel. The cross-flow ratio is defined as the ratio of cross-flow to inlet flow in the core is calculated and its variation due to a power surge can be analyzed. The flow rate range will not be so much of a problem as cross-flow is normalized to the inlet flow rate, but instead, parameters like temperature will affect the cross-flow variation. Figure 4-6 and Figure 4-7 show the variation of this ratio for a power surge of 1000 to 1450 MW_{th}. The first comment is that it takes some time to reach a new steady state once the power surge is simulated. Since it is an instantaneous large step of power, it is expected that the flow will oscillate a little bit before reaching its new level. Results show in both cases that the cross-flow magnitude tends to increase after the power surge. The higher in the core, the more the oscillations last before reaching a steady state for the new conditions.

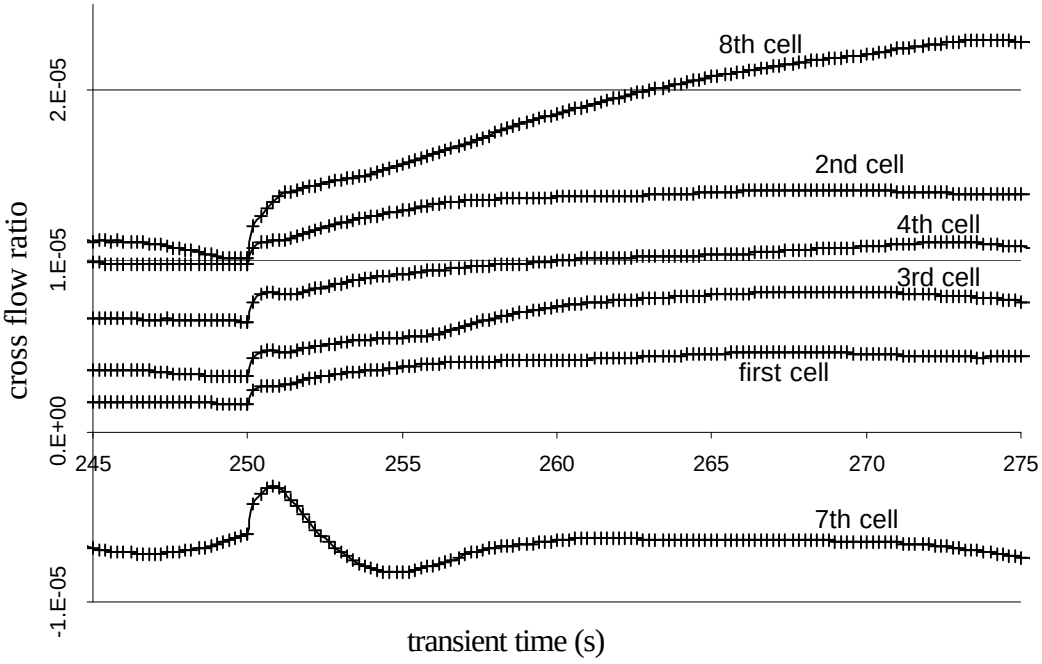

Figure 4-6: Cross-flow to inlet flow ratio for a 1000MW_{th} case. Cross-flow is from the Channel 1 to 2.

The figure 4-7 shows that for the seventh and the eighth cell, cross-flow takes longer to stabilize and has also more oscillations in the transient phase. However, for the bottom-core cross-flow junctions, the steady state is reached quite smoothly, but it still requires some time before the level of cross-flow stabilizes. As the temperature in the core is increasing with certain inertia, it is understandable that cross-flow, which also depends on the fluid properties, will reach its steady state conditions with a delay. Furthermore, it is logical that the flow through the top core cross-flow junctions would be disturbed, since it picks up perturbations from the lower part of the core.

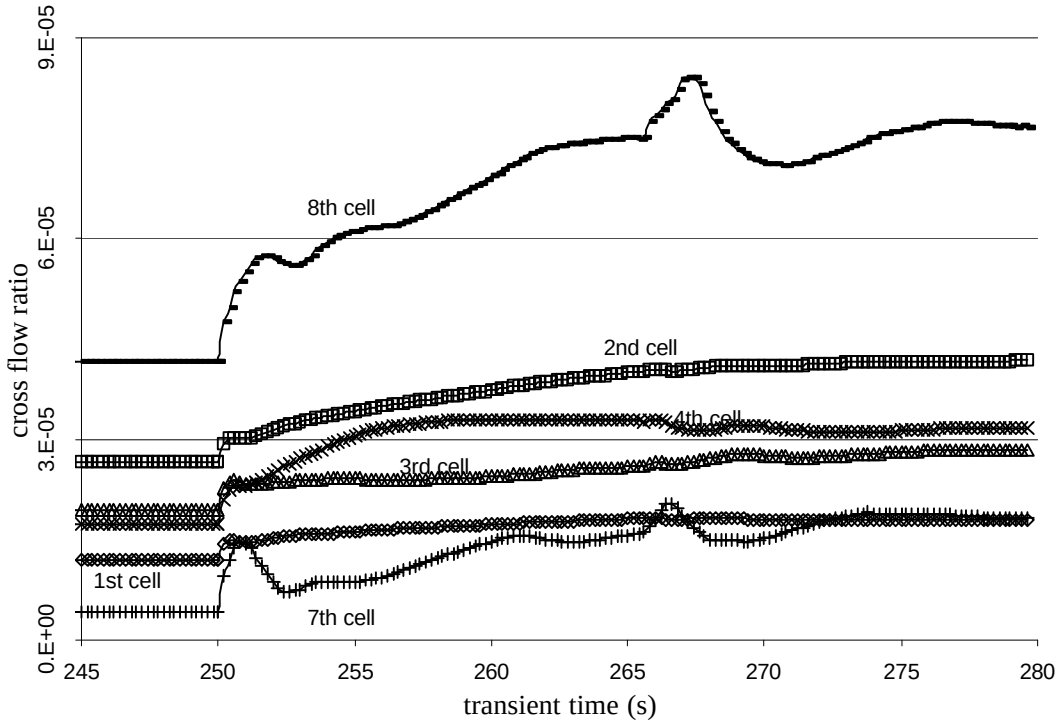

Figure 4-7: Cross-flow to inlet flow ratio for a 2443MW_{th} case. Cross-flow is from Channel 1 to 2.

Cross-flow phenomenon is now characterized with RELAP5. An expected result is that cross-flow increases as power increases. However, the cross-flow direction is not going in the expected way. As seen previously, the temperature distribution in the core

and the fluid velocity distribution should both push the flow inwards, due to density difference and pressure difference, even if these two phenomena have only a little effect due to the small differences in the distributions.

Cross-flow Between Two Adjacent Channels: FLUENT and RELAP5 Results

This part presents the results of cross-flow calculation in the simple system presented Chapter 3. This model has been developed to calculate cross-flow between two axial streams of fluid. This should allow doing an evaluation of the cross-flow model used in RELAP5. FLUENT and RELAP5 were used to calculate the cross-flow through an imaginary boundary inside a vertical pipe. The main interest is that, as we consider a system where the inner channel is an open channel, special model is needed in RELAP5, which is doing calculations using closed channels. This is the function of the so-called cross-flow junction. The geometry of the system is reminded in Figure 4-8.

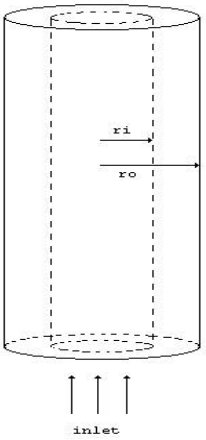

Figure 4-8: Two-sub channel pipe studied with FLUENT and RELAP5.

The first set of calculations is applied to a quite large system. The system is 5.0 m long, r_i=0.2m and r_o=0.4m.

Simulation in a Large-Diameter Vertical Pipe

The flow is expected to behave in a different manner whether its temperature remains constant or changes due to a power density. Indeed, the temperature of the fluid affects its energy, and the fluid properties may change consequently as its temperature increases. To analyze this effect, tests have been done with and without power. The results from FLUENT calculations presented in this paper show the solution obtained by the code on the calculation domain. So, the domain presented in all the following FLUENT figures is actually an elementary angular domain of the pipe like represented on Figure 3-3.

If no power is added to the fluid

The first test performed with this geometry was with a different inlet velocity in each of the imaginary channel. The velocity profile is described Figure 4-9, profile (a).

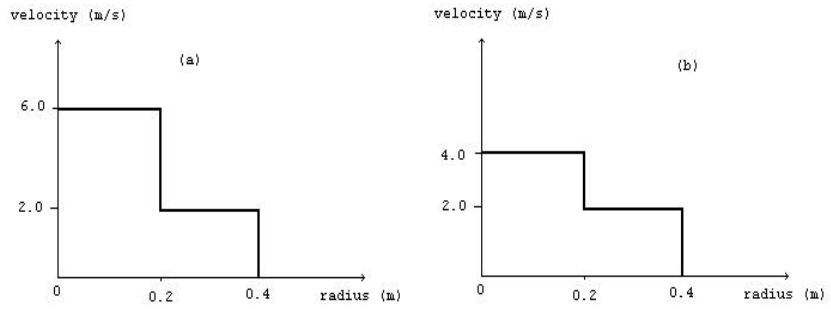

Figure 4-9: Inlet velocity profiles used in cross-flow simulation.

Two tests with different pipe length were performed. The first one was over a 50m long pipe. The grid on this area is a non-uniform mesh of 500 x 60 mesh points. The mesh is much finer in the regions of high gradients or of regions of interest. These are the central region at r=0.2m, and the entrance region. For these regions, GAMBIT allows

having a finer mesh by setting a ratio between the dimensions of adjacent cells.. As seen on Figure 4-10, this pipe is long enough such that the flow becomes fully developed. The evolution of axial velocity shape is displayed on Figure 4-10. The mixing length can be determined as the point where the flow gets his final shape that follows a one-seventh-power law. The radial velocity is the cross-flow velocity, and data at r=0.2 have been collected on a second run with the same boundary conditions, but on a shorter domain such that only the beginning of the mixing process appears. This second run was done only on a 0.4mx5.0m domain. The mesh grid for this simulation was a 500 x 40 orthogonal mesh. Figure 4-11 shows a more detailed view of the mixing process. Both plots represent a length of 5 meters. Figure 4-11 shows the calculation domain. This is actually an elementary angular domain of cylinder. The centerline is located at the bottom of the calculation domain, as explained previously.

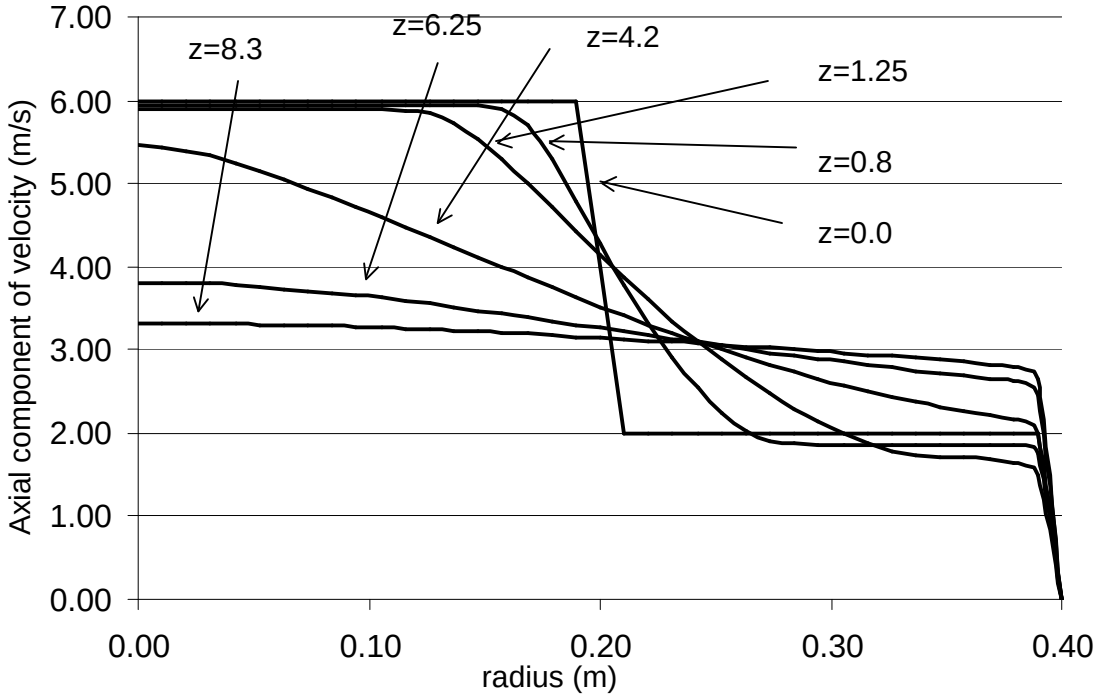

Figure 4-10: Axial evolution of the axial velocity profile. z is the height in meters.

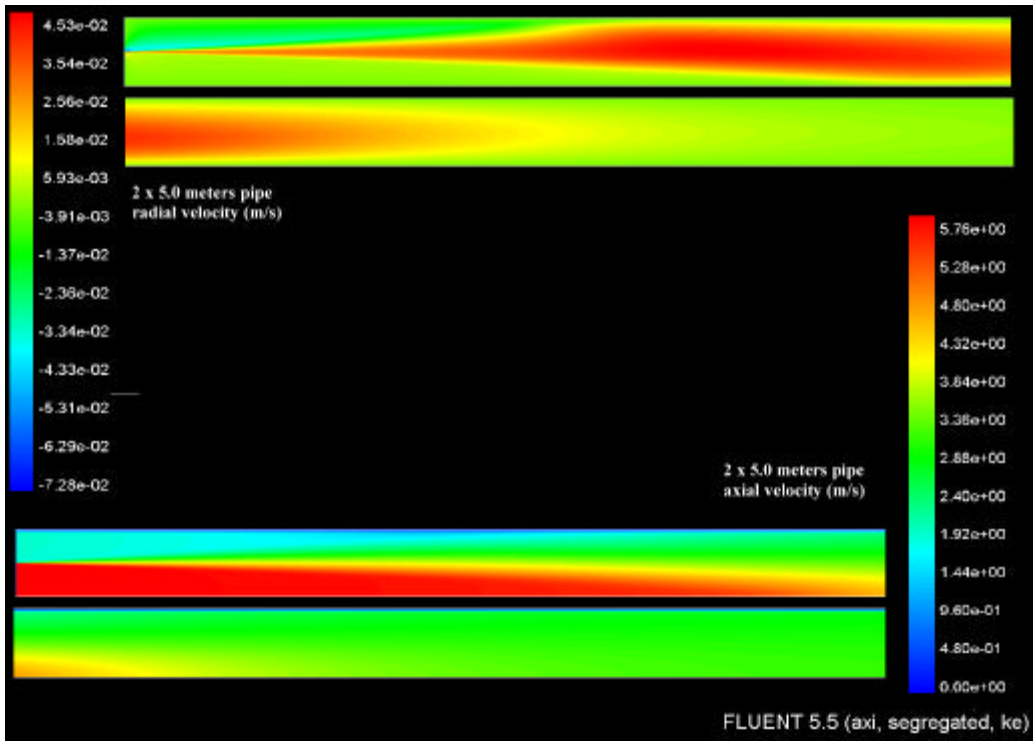

Figure 4-11: Radial (V-velocity) and axial (U-velocity) velocity distribution at the entrance of the tube for V_i=6.0 m/s and V_o=2.0 m/s.

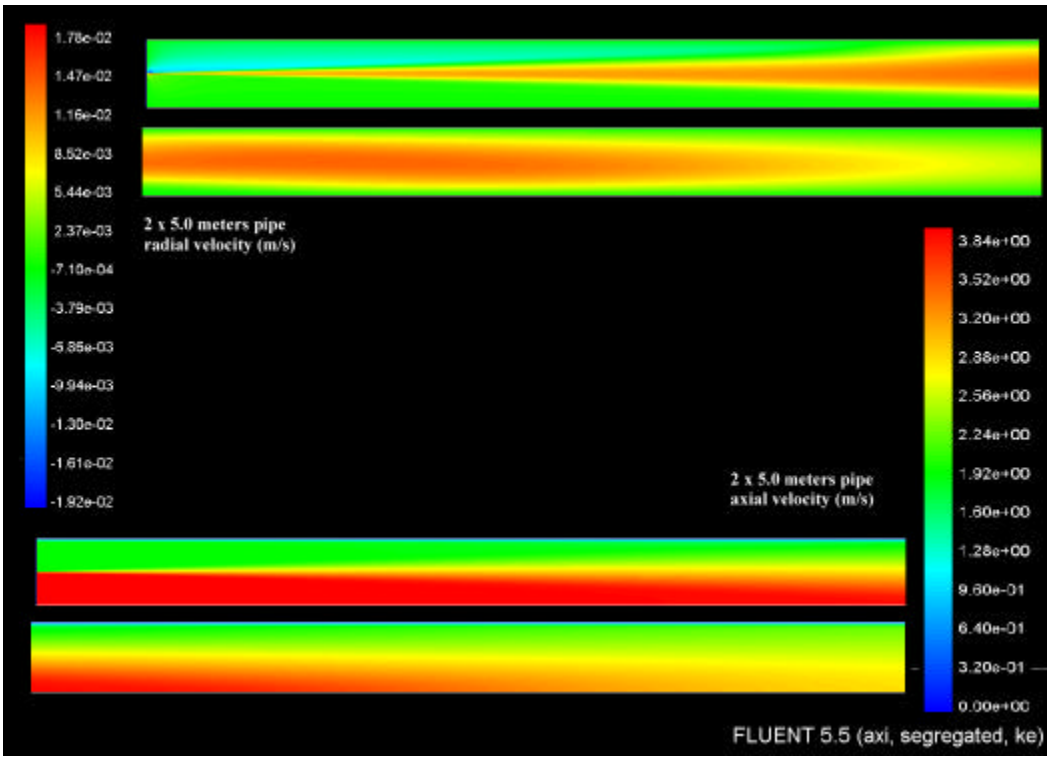

Figure 4-12: Radial (V-velocity) and axial (U-velocity) velocity distribution at the entrance of the tube for V_i=4.0 m/s and V_o=2.0 m/s.

The sign of the radial velocity shows two behaviors. First, the fluid at lower velocity, right at the entrance is attracted by the region of low velocity by pressure difference. Then, the fluid is going from the central part of the flow to the outer part. There is a transfer of momentum of the liquid from the high velocity part to the lower velocity region, and then, the fluid is moving outwards to reach the one seventh power law distribution as seen above.

The same simulation was realized with the inlet velocity profile (b), as shown on Figure 4-9, and results are shown Figure 4-12. With such a lower velocity, cross-flow intensity is strongly reduced. The attraction of fluid at the entrance (the blue region where radial velocity is negative) is less important in case of an inner velocity of 4 m/s (Figure 4-12) than for an inner velocity of 6 m/s (Figure 4-11).

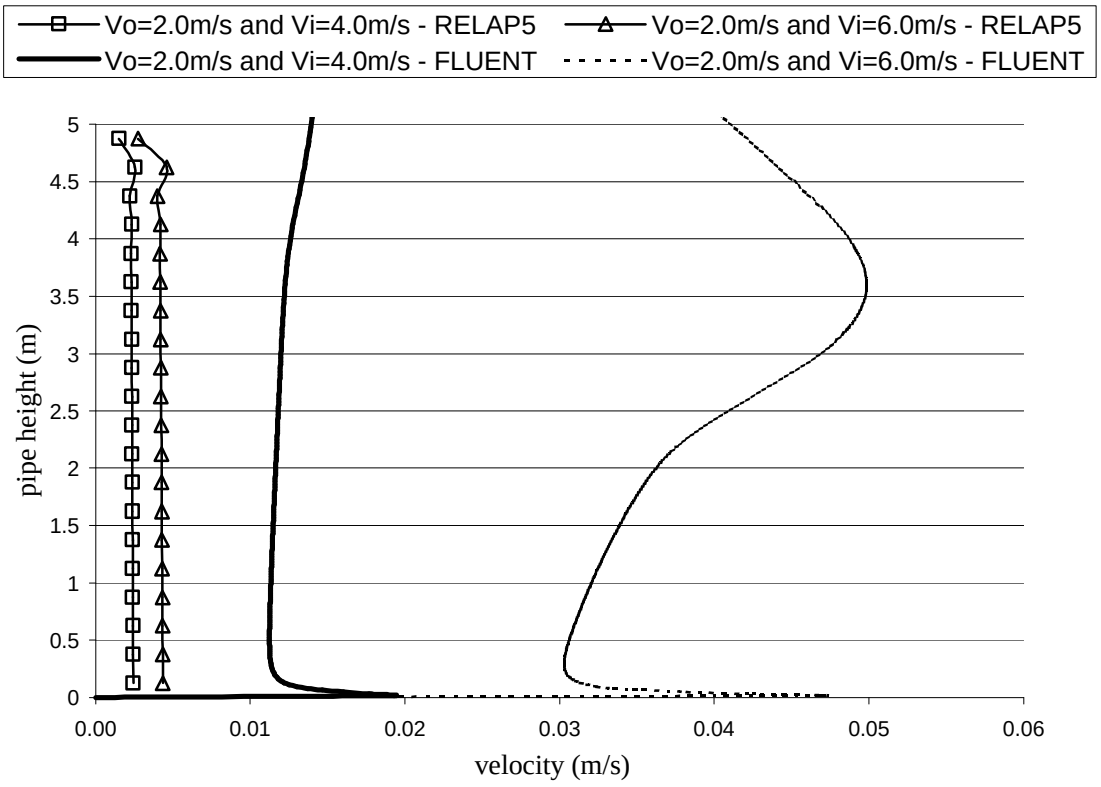

Figure 4-13: Comparison of cross-flow prediction between FLUENT and RELAP for two simulations.

Data got from these runs have been plotted and compared to the same conditions solved with RELAP5. Figure 4-13 shows the predictions of cross-flow with two different methods: RELAP5 and CFD with FLUENT.

There are differences between the predictions of cross-flow. Results are consistent as in average, cross-flow for the case where V_i is equal to 6.0 m/s is about 2.5 times the magnitude of cross-flow for an inner velocity of 4.0 m/s, but still, FLUENT prediction is about ten times larger than RELAP5 results. Also, RELAP5 does not predict the oscillations at the beginning of the pipe. This is explained by the fact that RELAP5 uses integrated quantities over a much larger volume than FLUENT, and these transient phenomena are then eluded. Other results concern the axial velocity and are presented on Figure 4-14.

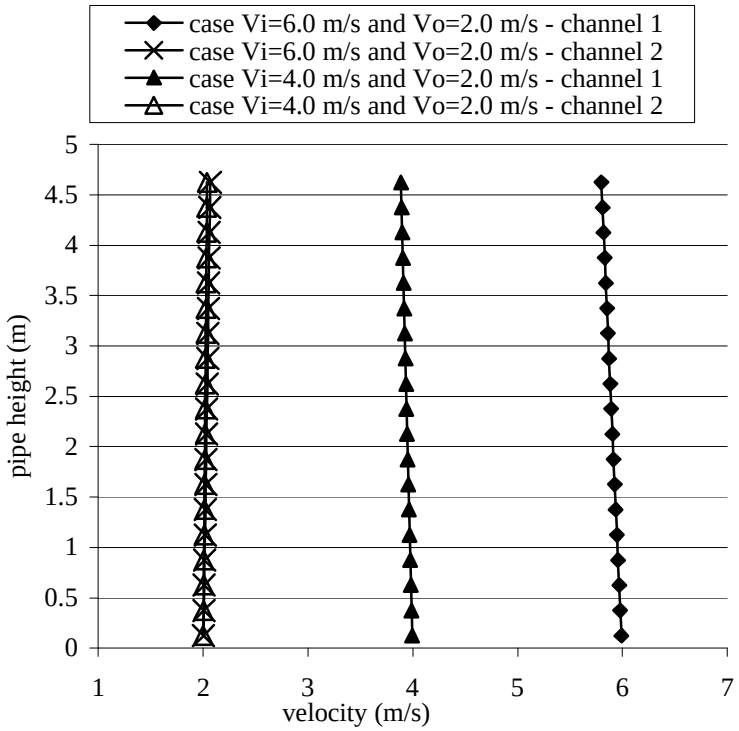

Figure 4-14: Evolution of the axial velocity for the two RELAP5 axial channels along the pipe, for the two inlet boundary conditions (a) and (b).

FLUENT predicts a mixing much faster than RELAP5. A weakness of RELAP5 is that it considers pipes as closed channels. Drag force from a channel stream to the other needs to be taken into account. Even with a low viscosity fluid, FLUENT predicts a mixing length much smaller than that. Cross-flow phenomenon is not treated with enough accuracy to calculate this problem.

If power is added to the fluid

The last situation studied with this specific geometry is the case of a channel where the fluid is entering at a constant velocity over the cross section area, but the central part of the channel is heated. The case was studied with a non-constant power density over the cross section of the pipe. The simulation presented here considers that the central channel is heated with a power density equal to 66.1 MW/m^3. The velocity of the fluid (water) entering the volume is 2.0 m/s everywhere.

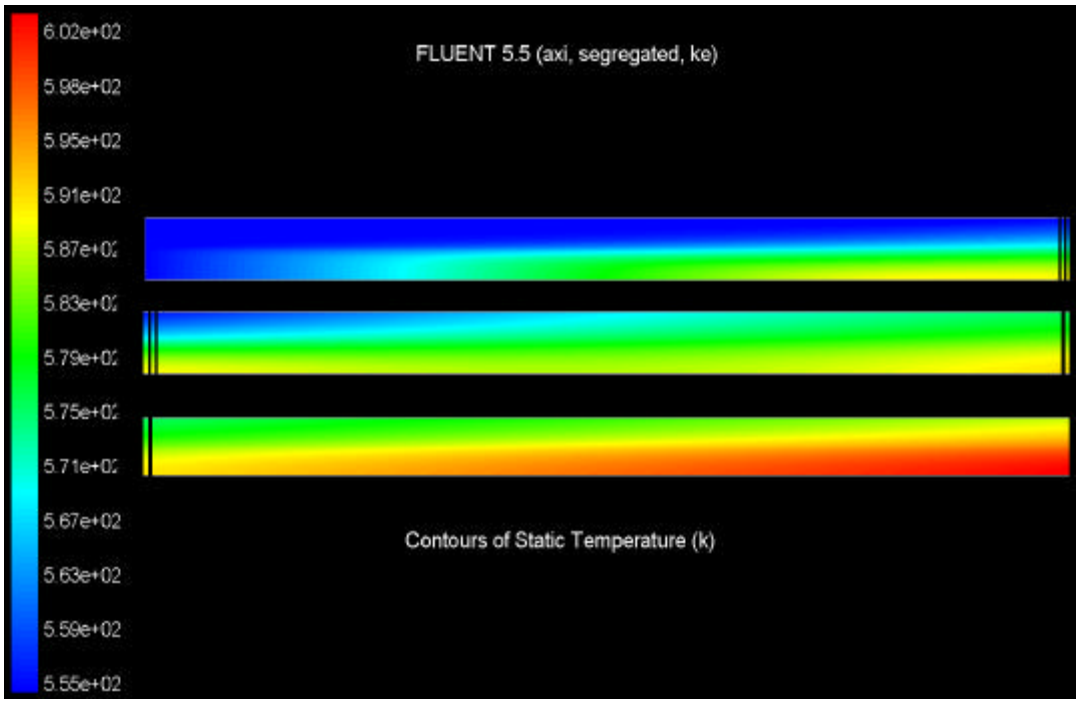

Figure 4-15: Temperature distribution over the total length of a 20.0 m pipe heated in the central channel at 66.1 MW/m^3.

Figure 4-15 shows the evolution of the temperature of the fluid as it goes all the way through a 20.0 meters long pipe, heated in its central part.

But the major interest is the cross-flow occurring due to the heating of the fluid. Figure 4-16 shows the results of the calculation of radial velocity in a shorter domain. The 5.0 meters pipe was discretized in a very fine mesh grid (40 x 500).

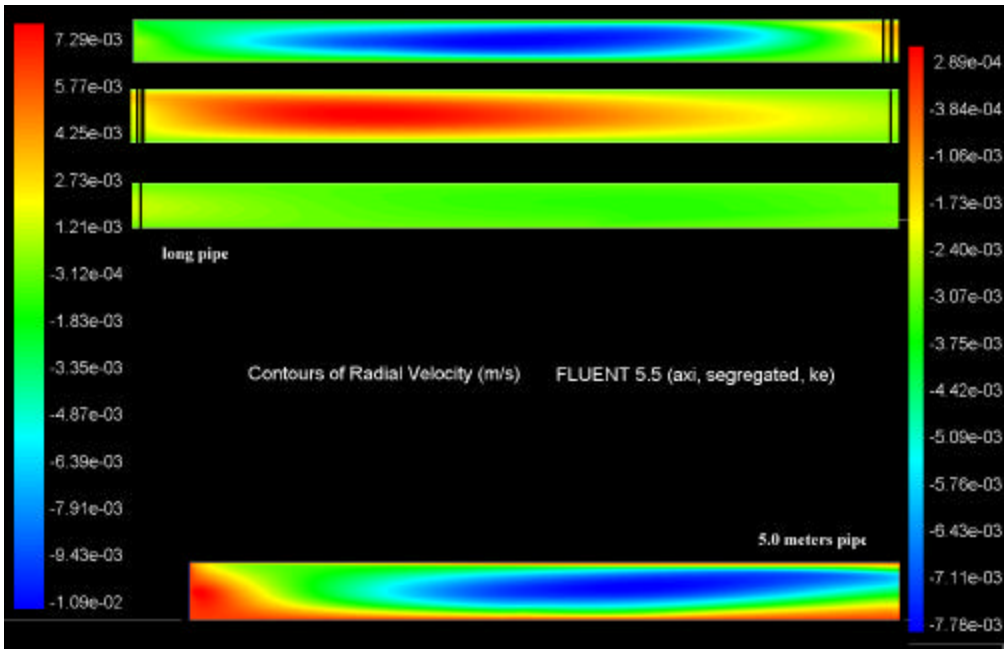

Figure 4-16: Radial velocity for a constant inlet velocity and a heated central channel.

On Figure 4-16, the first three pictures (and the scale on the left) represent the general behavior of the radial velocity along the 20.0 meters long pipe heated in the central channel. The fourth one focuses on the inlet region. Figure 4-17 shows the radial velocity at a radius of 20 cm (which corresponds to the interface between the two channels). These results have been obtained with FLUENT and RELAP5. The negative sign means that the fluid is moving from the outer channel to the inner channel. This is illustrated with the blue and green regions on Figure 4-16. This graph shows that both FLUENT and RELAP5 predict the same behavior of the cross-flow velocity at the

entrance of the pipe. However, there is a net difference of behavior of the predictions after that. The following Figure 4-18 shows that axial velocity is changing significantly as temperature increases. The density of the fluid heated in the central channel is becoming lower and lower and the velocity of the water increases.

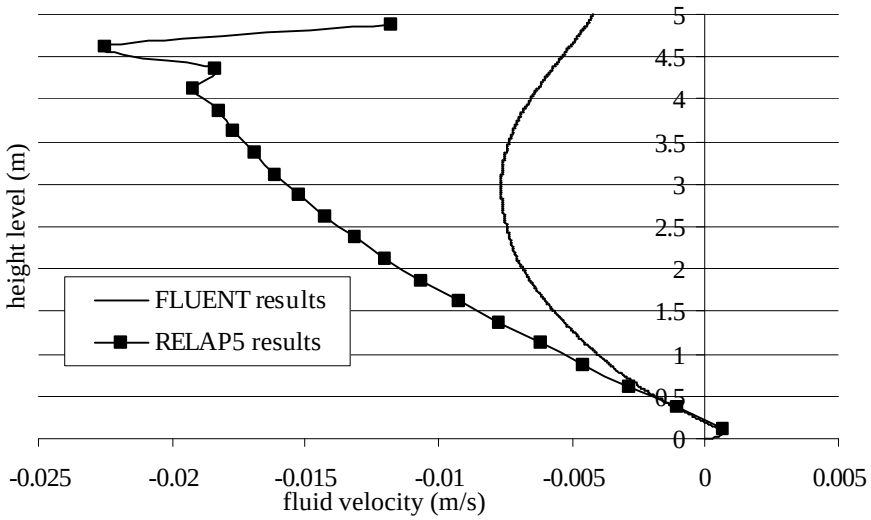

Figure 4-17: Cross-flow velocity at the artificial interface between the two channels.

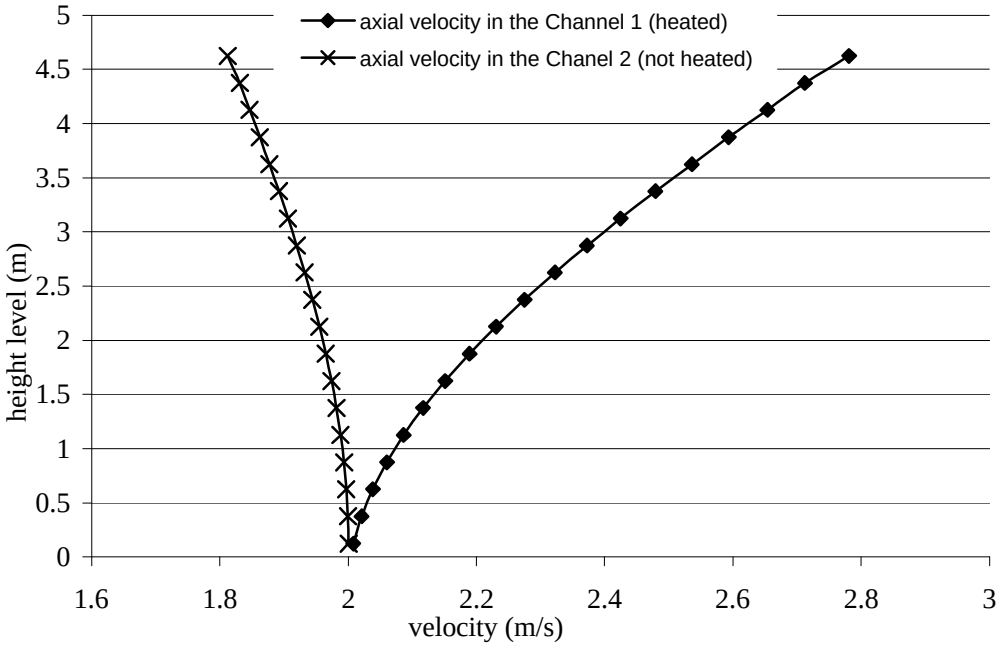

Figure 4-18: Axial velocity in Channel 1 (heated) and Channel 2 (non-heated)

Whereas RELAP5 does not predict a big change in the temperature of the fluid in the outer channel, FLUENT predicts a much faster heating of the second channel as seen on Figure 4-15. Water from the outer channel is attracted to the central stream, which explains the decrease of the axial velocity in the beginning of the pipe.

Simulation in a Small-Diameter Pipe

Similar tests were conducted with another set of domains. The principle is the same, but the diameter of the tubes was much smaller. For the geometry described on Figure 4-8, the tubes were 2 cm outer diameter. This means that r_o=1 cm and r_i = 0.5 cm. The first simulations were conducted without fluid heating. For these calculations, the mesh was composed of a 200 x 50 orthogonal grid.

If no power is added to the fluid

In this case where the power density for the heat source was zero, three different inlet velocity profiles were chosen. The outer channel axial inlet velocity was set equal to 2.0 m/s and three tests were done for inner channel velocity: 2.5 m/s, 4.0 m/s and 6.0 m/s. The Figures 4-19 and 4-20 show the prediction of axial and radial velocity for this experiment. The behavior of the flow is similar to the case of a large diameter pipe. However, as seen on Figure 4-21, cross-flow is lower for small diameter tubes. This is explained by the wall effect that acts to push the flow inwards. Small diameter tubes are more sensitive to this phenomenon. But this phenomenon was observed in a region close to the inlet of the tube, as farther, the same behavior is observed. RELAP5 tests have also been performed on the same geometry under the same conditions. Figure 4-22 shows the cross-flow velocity prediction for the three types of unheated calculations.

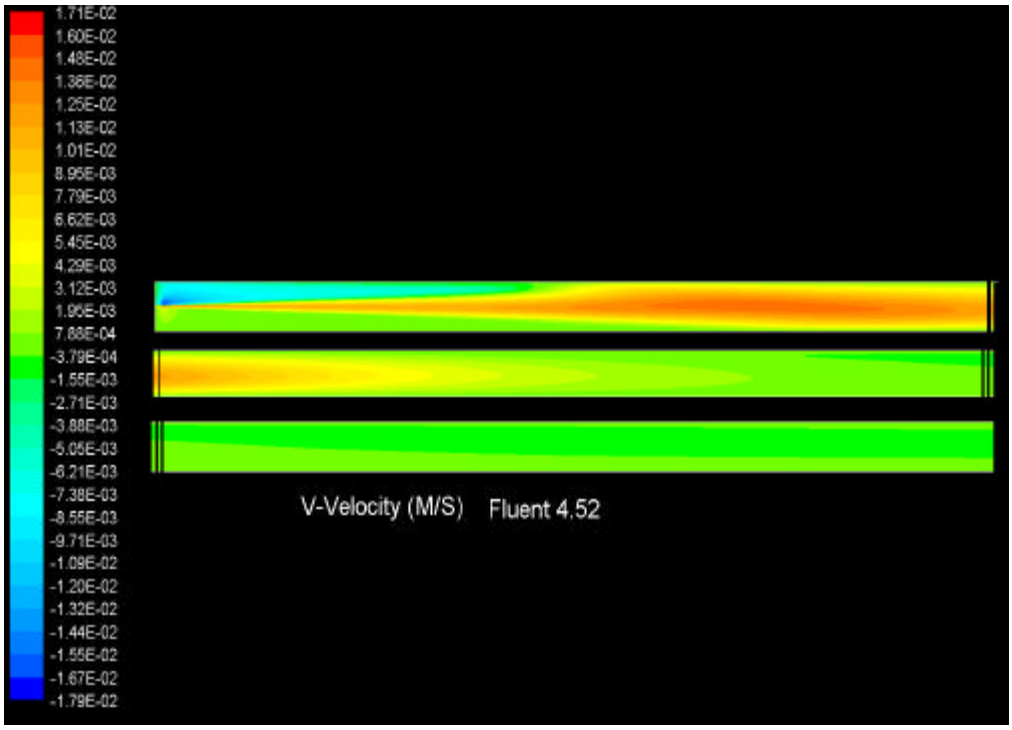

Figure 4-19: Radial velocity in a small size tube in an adiabatic flow. V_i=4.0 m/s and V_o=2.0 m/s.

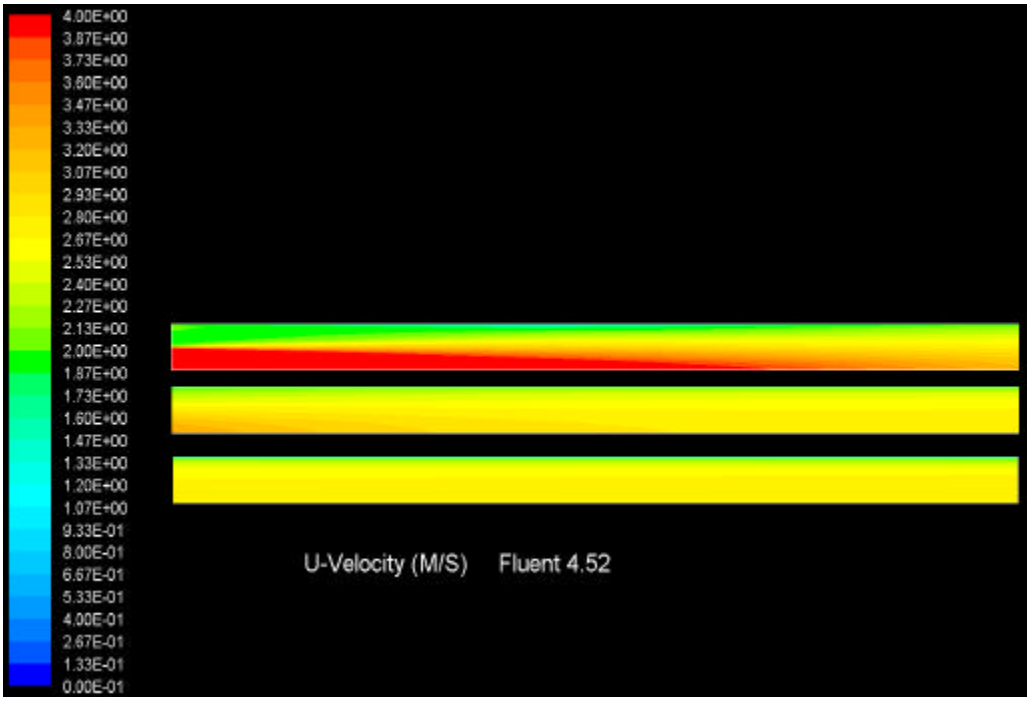

Figure 4-20: Axial velocity in a small size tube in an adiabatic flow. V_i=4.0 m/s and V_o=2.0 m/s.

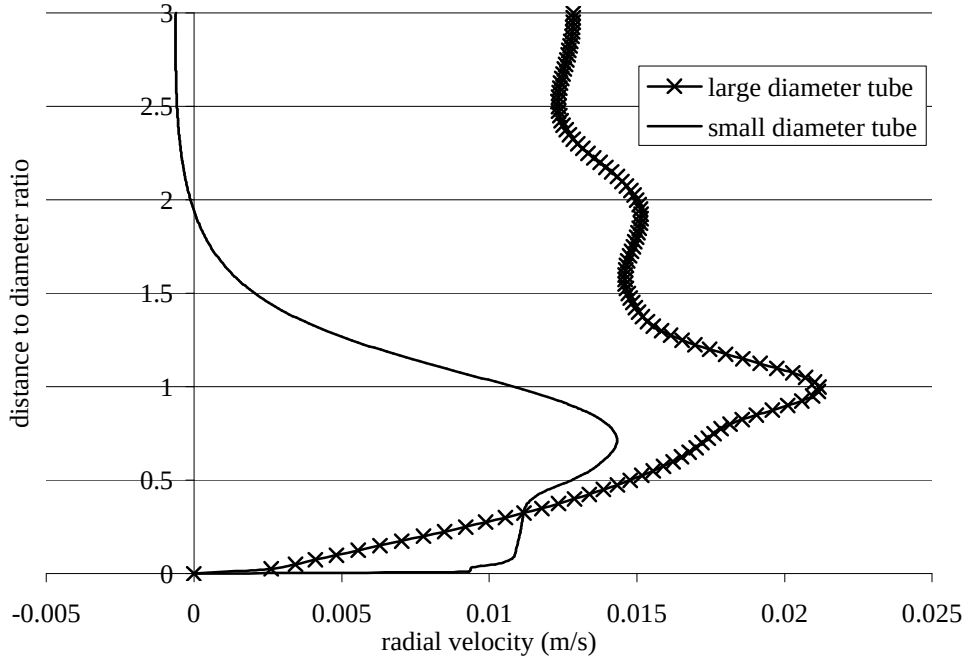

Figure 4-21: Cross-flow velocity versus distance to diameter ratio for large and small diameter tubes.

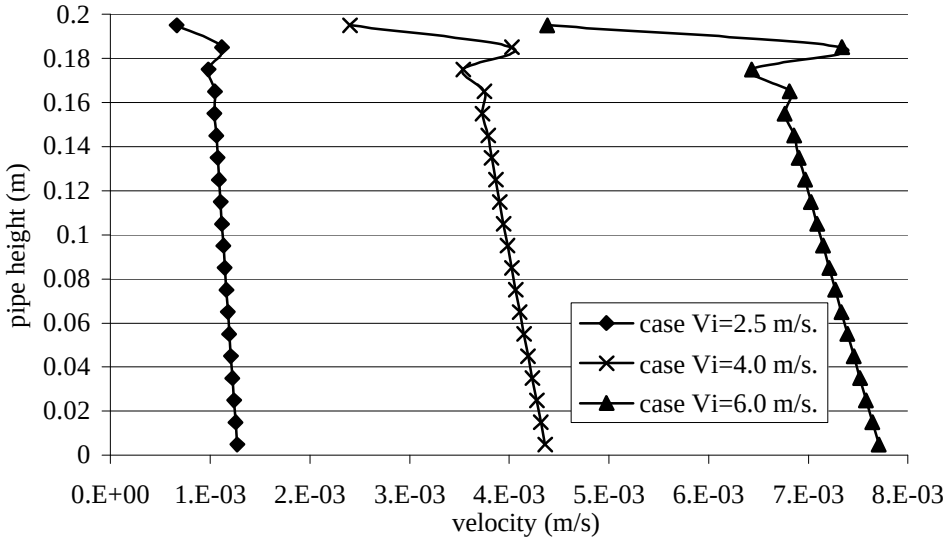

Figure 4-22: Cross-flow velocity for unheated small diameter channels (RELAP5 calculations).

Cross-flow is increasing as inner channel velocity is increasing. This is the general behavior expected from previous cases. However, the same comments can be

done concerning axial velocity. The RELAP5 predictions of axial velocity evolution show again that mixing is not occurring as fast as FLUENT predicts it. This is a problem in RELAP5 modelisation of cross-flow that has been discussed previously.

If power is added to the fluid

The effect of heating on flow evolution in the channel is obvious for small diameter channels too. Two different cases were run to observe the effect of heating. The first one was run with a very high power density, 600 MW/m^3, which makes a total power of 10 kW in the first channel, and no power in the second channel. Inlet velocities were taken equal to 2.0 m/s in both channels, and inlet temperature is still 555 K for a pressure of 15.68 MPa. And the second case has the same initial conditions, but power density is more realistic: the inner channel has a 160 MW/m^3 (2.7 kW for the total channel) and the outer channel has a 20 MW/m^3 (0.94 kW for the whole channel). As heat is transferred to the two channels, with a power density higher in the center than in the outer channel, the axial velocity increases in both channels. This phenomenon is calculated by RELAP5 and FLUENT. As inlet velocity is the same across the inlet area, the heating process and temperature increase induces cross-flow. Also cross-flow is more important in the case where power density difference in the tube is more important. As seen on Figure 4-23, cross-flow is much larger when the difference of power density between the two channels is the largest.

Steam flow

Previous cases were considering pure liquid flows. This case shows an example with superheated steam. No heating occurs along the path, but initial velocities are set much higher. The inner channel initial velocity is equal to 40.0 m/s and the outer channel

initial velocity is 20.0 m/s. A pressure of 10 bar was used (10^6 Pa), and the inlet temperature is 520 K. Calculations done with RELAP5 show that cross-flow velocity is higher in the case of steam flow, and the mixing is faster (Figure 4-24).

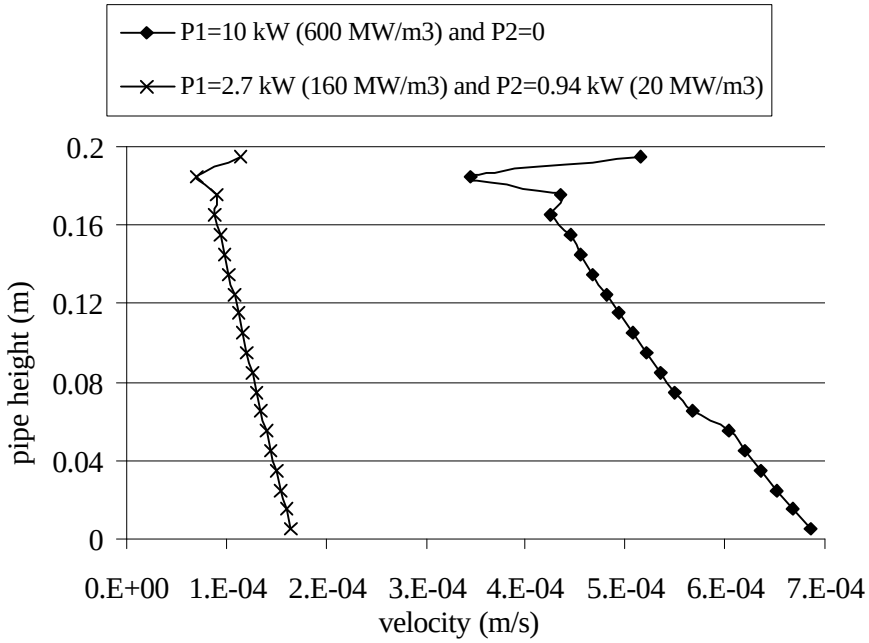

Figure 4-23: Cross-flow velocity between heated small diameter channels.

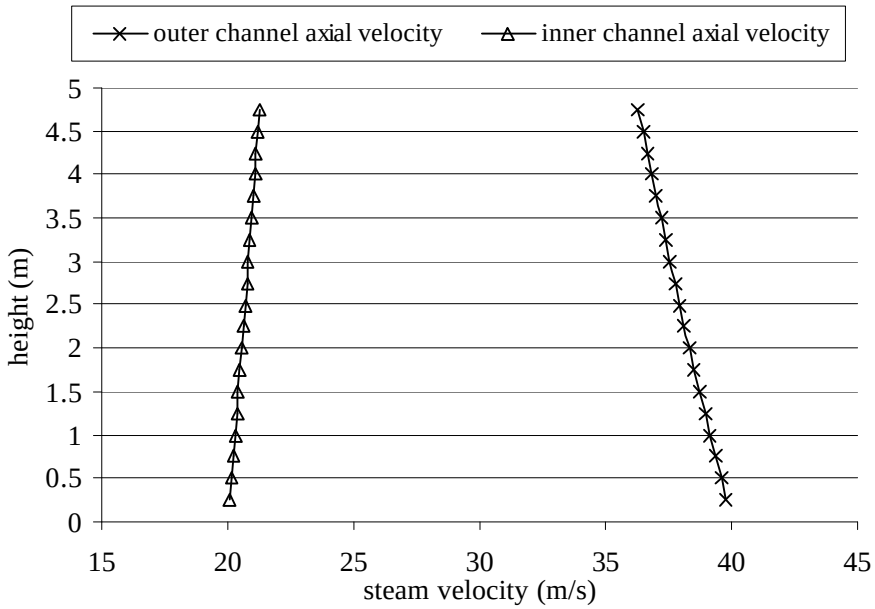

Figure 4-24: Axial velocity distribution for superheated steam.

Conclusions and Recommendations

The study showed that cross-flow is an important concern in modeling nuclear reactor cores. A series of calculations under different flow conditions have demonstrated that the magnitude of cross-flow varies with inlet flow and temperature conditions as well as the velocity and temperature axial gradients. It was shown that both velocity and temperature gradients have significant effect on the magnitude of the cross-flow.

Results of the study have shown the lack of sufficient accuracy of the RELAP5 cross-flow model even for cases involving single-phase flow and simple geometry. Although high resolution CFD allows for high accuracy prediction of cross-flow, it cannot be used to model large portion of a reactor core. The number of computational mesh points to resolve a full reactor core would be in excess of billions that is far beyond the current computational capability of the most advanced computer systems.

Results of the study have shown the limitations of RELAP5 to model multi-dimensional flow and heat transfer problems. These limitations were illustrated by the calculation of the radial velocity in the cross-flow junctions. The close-channel treatment of the flow in the reactor core, which completely ignores the cross-flow, is a less desirable solution. In RELAP5 model because the advection terms are neglected in the momentum equation, there is no transport of axial momentum in the radial direction. As a result, using a simple loss factor RELAP5 treats losses in the transverse direction. This is obviously a crude approximate

Along with the cross-flow junction comes the problem of stress between fluid layers. In a problem like the one treated in this study, shear stress between streams of fluid is important. Especially when axial velocities are different, viscosity phenomenon

will play an important role in defining the shape of the flow. In reactor cores, special attention is needed to model cross-flow in presence of fuel rod bundles that partially obstruct radial flow motion. The primary concern is to find a proper loss factor that would be used as a wall loss factor to model friction between vertical layers of flow in different channels. Another issue is the proper modeling of the turbulence effect on cross-flow calculation. In nuclear reactor cores, cross-flow is also influenced by all the equipment and core components that are used to divert the flow from its initial path to provide better mixing and homogenization of flow parameters.

The study was conducted for a purely single-phase flow where the contribution of cross-flow under uniform flow and thermal conditions is insignificant. In two-phase flow systems, the relative contribution of cross-flow is much more significant. Further studies are needed to evaluate the RELAP5 modeling capability for analysis of two-phase flow and heat transfer in open channels of light water reactors. The use of high resolution CFD model proved valuable in calculating cross-flow across parallel channels. Future studies should address both cross-flow modeling and empirical relations that are used to account for loss of momentum in transverse direction in one-dimensional codes like RELAP5.

In summary, RELAP5 is a widely used thermalhydraulic code, but this study has shown that cross-flow results need to be interpreted with caution because the model used is not accurate. Cross-flow modeling in RELAP5 has to be improved to consider actual three-dimensional effects. Models could be developed using CFD calculations.

APPENDIX A
SUMMARY OF SCDAP/RELAP5 HYDRODYNAMIC COMPONENTS

Table A-1: Hydrodynamic components used to build the reactor model.

Component Number	Component type	Feature
100	Pipe	Upper annulus
102	Branch	Inlet annulus
104	Pipe	Downcommer
106	Branch	Lower head
108	Branch	Lower plenum
111	Pipe	Core channel 1
112	Pipe	Core channel 3
113	Pipe	Outer core channel
114	Pipe	Core channel 2
115	Pipe	Core channel 4
118	Pipe	Core bypass
14X	Single junction	Connect 111MM to 114MM
08X	Single junction	Connect 112MM to 115MM
12X	Single junction	Connect 114MM to 112MM
13X	Single junction	Connect 115MM to 113MM
151	Branch	Upper plenum center 1
152	Branch	Upper plenum center 2
153	Branch	Upper plenum center 3
154	Branch	Upper plenum center 4
161	Branch	Upper plenum middle 1
162	Branch	Upper plenum middle 2
163	Branch	Upper plenum middle 3
164	Branch	Upper plenum middle 4
171	Branch	Upper plenum outer 1
172	Branch	Upper plenum outer 2
173	Branch	Upper plenum outer 3
174	Branch	Upper plenum outer 4
181	Single volume	Control assembly housing
182	Single volume	Control assembly housing
183	Single volume	Control assembly housing
190	Branch	Upper head

Table A-2: Hydrodynamic components in the steam generator.

Component Number	Component type	Feature
X66	Time dep. volume	Sg feedwater
X67	Time dep. Junction	Sg feedwater
X70	Single volume	Sg upper downcommer
X72	Branch	Sg inlet downcommer
X74	Pipe	Sg downcommer
X75	Single junction	Sg boiler
X76	Pipe	Sg boiler
X78	Separator	Sg swirl vanes
X80	Branch	Sg dryer
X82	Single volume	Sg dome
X84	Branch	Sg steam line
X85	Valve	Sg steam outlet
X86	Time dep. Volume	Steam outlet
X87	Valve	Sg porv
X88	Time dep. Volume	Safety container
X89	Valve	Sg safety valve
X90	Time dep. Volume	Safety container

Table A-3: Hydrodynamic components of the primary loop.

Component Number	Component type	Feature
X00	Pipe	Hot leg vessel outlet
X02	Branch	Hot leg pressurizer
X03	Single junction	Hot leg stop
X04	Single volume	Hot leg sg inlet
X06	Branch	Sg primary coolant inlet
X08	Pipe	Sg tube sheet
X10	Branch	Sg primary coolant outlet
X12	Pipe	Pump suction pipe
X14	Pump	Primary loop pump
X16	Single volume	Cold leg pump outlet
X17	Single junction	Cold leg stop
X18	Single volume	Cold leg ECC1
X20	Branch	Cold leg ECC2
X22	Single volume	Cold leg vessel inlet

Table A-4: Hydrodynamic components of the pressurizer.

Component Number	Component type	Feature
440	Branch	Pressurizer dome
441	Pipe	Pressurizer tank
442	Single junction	Junction hot leg/surge line
443	Pipe	Surge line
444	Valve	Pressurizer porv
445	Valve	Pressurizer safety valve
449	Single volume	Container

APPENDIX B
RELAP5/SCDAP HEAT STRUCTURES FOR THE CORE AND STEAM GENERATOR

Table B-1: Heat structures in the core and the steam generator.

Heat struct. Number	Feature
X001	Hot leg piping
X061	s.g. inlet plenum
X062	s.g. partition plate
X081	s.g. tubes
X082	s.g. tubesheet
X101	s.g. outlet plenum
X121	s.g. pump suction plenum
X161	Cold leg piping
X701	s.g. upper shell
X721	s.g. middle shell
X741	s.g. shell base
X742	s.g. lower shell
X761	s.g. lower wrapper
X781	s.g. upper wall/swirl vane
X821	s.g. shell top
1001	Upper Head
1002	Upper vessel wall
1003	Middle vessel wall
1004	Lower vessel wall
1041	Thermal shield
1061	Lower head structures
1071	Lower support plates
1081	Lower plenum structures
1151	Core baffle
1201	Core barrel
1501	Center channel upper plenum structures
1601	Middle channel upper plenum structures
1701	Outer channel upper plenum structures
1811	Center channel control housing
1821	Middle channel control housing
1831	Outer channel control housing
1851	Upper support plate
1901	Upper head structures

APPENDIX C
RELAP5 INPUTS FOR THE TWO-CHANNELS SYSTEM

This appendix presents the RELAP5 inputs used to model the single pipe with taking into account the cross-flow phenomenon.

```
=two channel test
100 new stdy-st
102 si si
201 400.0 1.0e-6 0.05 3 50 200 200

506   time       0    gt   null   0      1000.0  l * for power

0880000 botin tmdpvol
0880101 7.854e-5 1.0e+02 0.0 0 90.0 1.0e+2 0 0 0
0880200 3
0880201 0.0 1.56821e+7 555.0

0980000 botout tmdpvol
0980101 2.356e-4 1.0e+02 0.0 0 90.0 1.0e+2 0 0 0
0980200 3
0980201 0.0 1.56821e+7 555.0

0890000 junin tmdpjun
0890101 088010002 100010001 7.854e-5
0890200 0
0890201 0.0 2.0 2.0 0.0
0890202 1.0e+06 2.0 2.0 0.0

0990000 junout tmdpjun
0990101 098010002 110010001 2.356e-4
0990200 0
0990201 0.0 2.0 2.0 0.0
0990202 1.0e+6 2.0 2.0 0.0

*inlet channel
1000000 channel1 annulus
1000001 20
1000101 7.854e-5 20
1000301 0.01 20
1000601 90.0 20
1000801 0 0.01 20
1001001 0 20
1001101 0 19
1001201 3 1.58e+7 550.0 0 0 0 20
1001300 0
1001301 2.0 2.0 0.0 19

*outlet channel
1100000 channel2 annulus
1100001 20
1100101 2.356e-4 20
1100301 0.01 20
1100601 90.0 20
1100801 0 0.01 20
1101001 0 20
1101101 0 19
1101201 3 1.58e+7 550.0 0 0 0 20
1101300 0
1101301 2.0 2.0 0.0 19

*crossflow junction
1120000 crfl mtpljun
1120001 20 0
1120011 100010004 110010003 3.1416e-4 0.0 0.0 00003
+ 1.0 1.0 1.0
+ 10000 10000 0 20
1121011 0.0 0.0 20

*sngljun in
1200000 junin sngljun
1200101 100200002 130000000 7.854e-5 0.0 0.0 0 1.0 1.0
1.0
1200201 0 2.0 0

*sngljun out
1210000 junout sngljun
1210101 110200002 131000000 2.356e-4 0.0 0.0 0 1.0 1.0
1.0
1210201 0 2.0 0

*outlet-in tmdpvol
1300000 outin tmdpvol
1300101 7.854e-5 1.0e+2 0 0 90.0 1.0e+2 0 0 0010
1300200 3
1300201 0.0 1.568e+7 555.0

*outlet-out tmdpvol
1310000 outout tmdpvol
1310101 2.356e-4 1.0e+2 0 0 90.0 1.0e+2 0 0 0010
1310200 3
1310201 0.0 1.568e+7 555.0

*  heat structure inner channel
11000000  20  2  2  0  0.005
11000100  0  1
11000101  1  0.006
11000201  5 1
11000301  1.0 1
11000400  0
11000401  555.0 2
11000501  100010000 10000  1  1  0.01  20
11000601        0     0  0  1  0.01  20
11000701  10  0.05  0  0  20
11000801  0.01  10.0  10.0  0.0  0.0  0.0  0.0  1.0  20

*  heat structure outer channel
11100000  20  2  2  0  0.0087
11100100  0  1
11100101  1  0.0097
11100201  5 1
11100301  1.0 1
11100400  0
11100401  555.0 2
```

```
11100501  110010000 10000  1  1  0.01  20
11100601         0     0  0  1  0.01  20
11100701  11  0.05  0  0  20
11100801  0.015  10.0  10.0  0.0  0.0  0.0  0.0  1.0  20

*conduction between the channels
11120000 20 2 2 0 0.005
11120100 0 1
11120101 1 0.006
11120201 004 1
11120301 0.0 1
11120499 555.0 2
11120501 100010000 10000 1 1 0.01 20
11120601 110010000 10000 1 1 0.01 20
11120701 0 0.0 0 0 20
11120801 0.01 10.0 10.0 0.0 0.0 0.0 0.0 1.0 20
11120901 0.03 10.0 10.0 0.0 0.0 0.0 0.0 1.0 20

* general tables
*thermal properties for water
20100400 tbl/fctn 1 -1
20100401 523.0 0.635
20100402 548.0 0.6034
20100403 573.0 0.5617
20100404 598.0 0.5086

20100451 2.24e+6
20100452 2.312e+6
20100453 2.341e+6
20100454 2.313e+6
*  stainless steel
20100500  s-steel

* table of time, core power
20201000 power 506
20201001  0.0  10000.0 1.0e+6 10000.0
20201100 power 506
20201101  0.0      0.0 1.0e+6     0.0
.
```

LIST OF REFERENCES

1. W. WANG, "CFD Mixing analysis of vortex generator jets injected into confined cross-flow in rectangular duct," *Tuijin Jishu/Journal of Propulsion Technology* 19, 2 (1998).

2. P. AJERSCH, J.-M. ZHOU, S. KETLER, M. SALCUDEAN, I. S. GARTSHORE, "Multiple jets in a cross-flow: Detailed measurements and numerical simulations," *American Society of Mechanical Engineers (Paper)* (1995).

3. V. KASSERA, "Three dimensional CFD-analysis of tube vibrations induced by cross-flow," *4th International Symposium on Fluid-Structure Interactions, Aeroelasticity, Flow-Induced Vibrations and Voice ASME, Aerospace Division AD,* **53-2** (1997).

4. SCADP/RELAP5 Development Team, "SCDAP/RELAP5/MOD3.2 Code Manual Volume I: SCDAP RELAP5 Interface Theory," NUREG/CR-6150, INEL-96/0422, INEL, Idaho Falls (October 1997).

5. RELAP5 Code Development Team, "RELAP5/MOD3 Code Manual Volume I: Code Structure, System Models and Solution Methods," NUREG/CR-5535, INEL-95/0174, INEL, Idaho Falls (June 1995).

6. SCADP/RELAP5 Development Team, "SCDAP/RELAP5/MOD3.2 Code Manual Volume III: User's Guide and Input Manual-Appendix A," NUREG/CR-6150, INEL-96/0422, INEL, Idaho Falls (November 1997).

7. "FLUENT 5 User's Guide, Volume 2," Fluent Inc., Lebanon (July 1998).

8. "FLUENT 5 User's Guide, Volume 3," Fluent Inc., Lebanon (July 1998).

9. "FLUENT 5 User's Guide, Volume 1," Fluent Inc., Lebanon (July 1998).

10. "FLUENT 5.5 UDF User's Guide," Fluent Inc., Lebanon (September 2000).

11. "FLUENT 5 User's Guide, Volume 4," Fluent Inc., Lebanon (July 1998).

12. W. RODI, Turbulence models and their application in hydraulics, A state-of-the-art review, IAHR/AIRH, Rotterdam (1993).

13. W.K. GEORGE, R. ARNDT, Advances in Turbulences, Hemisphere Publishing International, New York (1989).

14. S.V. PATANKAR,. D.B. SPALDING, Heat and Mass Transfer in Boundary Layers, Applied Mathematics and Mechanics, Vol 15, Academic Press, New York (1994).

15. H. SCHLICHTING, Boundary Layer Theory, McGraw Hill, New York (1969).

16. B.E. LAUNDER, D.B. SPALDING, Lectures in Mathematical Models of Turbulence, Academic Press, London, England (1972).

17. D. CHOUDHURY, "Introduction to the Renormalization Group Method and Turbulence Modeling," Technical Memorandum TM-107, Fluent Inc., Lebanon (1993).

18. T. -H. SHIH, W. W. LIOU, A. SHABBIR and J. ZHU, "A new k-epsilon eddy viscosity model for high Reynolds number turbulent flows – Model development and validation," *Computer Fluids* 24, 3 (1995).

19. P. SPALART, S. ALLMARAS, "A one-equation turbulence model for aerodynamic flows," Technical Report AIAA-92-0439, American Institute of Aeronautics and Astronautics, New York (1992).

20. U. GRIGULL, J. STRAUB, P. SCHIEBNER, Steam Tables in SI Units, Springer-Verlag, New York (1990).

BIOGRAPHICAL SKETCH

Vincent Roux was born on May 25, 1977, in Périgueux, France. He graduated from Girault de Borneil High School in France. He entered the National School for Physics in Grenoble in the fall of 1997. As part of an academic exchange, he entered the University of Florida in the fall of 1999 as a graduate student, and obtained his French engineer diploma in Summer 2000. Since then, he has been pursuing a Master of Science degree in nuclear engineering sciences while working at INSPI as a graduate research assistant.